Design and Fabrication of Biodegradable Microfluidic Platforms for Enhanced Tunnelling Magnetoresistance Sensor

Paria Kamkar

Submitted in fulfilment of the requirements for the

Degree of Master in Research

Supervisors: Dr. Roghaieh Parvizi

James Watt School of Engineering

College of Science and Engineering

University of Glasgow

May 2025

Abstract

Cancer remains a significant global health issue with its incidence and mortality rates increasing rapidly worldwide. Therefore, detecting cancer at an early stage can significantly increase survival rates. However, conventional diagnostic methods often depend on bulky, expensive equipment and require trained personnel, which limits their accessibility. This underscores the urgent need for simple, low-cost diagnostic devices that enable timely and effective early diagnosis. Microfluidics is a technology for controlling fluids at the microscale with high accuracy has emerged as a powerful potential instrument in biomedical and environmental processes, particularly when combined with cutting-edge sensing technologies and eco-friendly materials.

In this contribution, we investigated the design and fabrication of biodegradable microfluidic devices to improve the performance of tunnelling magnetoresistance (TMR) sensors by utilizing the biocompatibility of hydrogels, such as Polyethylene Glycol Diacrylate (PEGDA) and Gelatin Methacryloyl (GelMA), in conjunction with Polydimethylsiloxane (PDMS). Through photolithography and digital light processing three-dimensional (3D) bioprinting, we obtained high-resolution microchannel geometries, where PEGDA exhibited the best fidelity and printability.

In this study, channels with a width of 500 µm and a depth of 1 mm were fabricated successfully using a 25% PEGDA solution. Optimal fabrication was achieved after modifying the layer height settings of the CELLINK Lumen X DLP 3D printer from the initial 100 µm to 50 µm and subsequently to 20 µm. The platforms were validated using TMR sensors for detecting magnetic nanoparticles (MNPs) in the concentration range of 0 to 40 × 10^3, showing a linear response with R^2 = 0.9771, indicating high sensitivity, reproducibility, real-time detection, and repeatable recovery of the baseline. These results underscore the potential of PEGDA- and PDMS-based biodegradable microfluidic devices for scalable biosensing applications. The integration of magnetic biosensing, hydrogel-assisted microfabrication, and sustainable materials enables the development of next-generation diagnostic tools that are not only efficient and sensitive but also environmentally friendly and well-suited for point-of-care testing and home-based monitoring.

Table of Contents

List of Tables

List of Figures

Acknowledgement

I would like to express my heartfelt gratitude to my supervisors, Dr. Roghaieh Parvizi and Professor Hadi Heidari, for their invaluable guidance, unwavering support, and kind encouragement throughout the past year. Their deep knowledge, patience, and thoughtful critiques have shaped this work in countless ways. I am truly grateful for their mentorship and the trust they placed in me during this journey.

I am also sincerely thankful to Dr. Tahereh Azargoshasb for her generous support in every aspect of this journey, whether intellectually, emotionally, or personally. Her kindness, wisdom, and encouragement have meant a great deal to me, and I truly value her as both a mentor and a person.

My sincere thanks also go to Ali Mokhtarzadeh and Yuanxi Cheng (Kevin) for their valuable technical support and shared knowledge, both of which were essential throughout the course of this work.

Special thanks to all members of the meLAB research group for creating a supportive and stimulating environment that greatly contributed to my learning and progress.

My heartfelt appreciation goes to my loved spouse and my parents, whose unwavering love, patience, and support have been my source of strength during this journey. Their constant encouragement has meant the world to me.

Author's Declaration

I, the undersigned, hereby declare that this thesis is entirely my own work and has been written in my own words. All sources used during the research have been fully acknowledged, and all quotations properly cited. This thesis has not been submitted, in whole or in part, for the award of any other degree or diploma at this or any other institution.

I understand the ethical responsibilities related to my research, and I confirm that this work complies with the requirements of the University of Glasgow and the relevant Research Ethics Committee.

Signature: Paria Kamkar

Date: 09.05.2025

List of Abbreviations

2D	Two-dimensional
2PP	Two-Photon Polymerization
3D	Three-dimensional
4D	Four-Dimensional
°C	Degrees Celsius
ρ	Fluid density
p	Pressure
μ	Dynamic viscosity
μg	Micro gram
μM	Micrometre
μPADs	Microfluidic Paper-based Analytical Devices
μTAS	Micro Total Analysis System
AI	Artificial Intelligence
AMR	Anisotropic Magnetoresistance
APS	Poly (1,3-diamino-2-hydroxypropane-co-polyol sebacate)
BoC	Biosensors-on-Chip
CFU	Colony-Forming Unit
CMOS	Complementary Metal-Oxide-Semiconductor
Co	Cobalt
COC	Cyclic Olefin Copolymer
COVID-19	Coronavirus disease 2019
Cu	Copper
Cr	Chromium
CV	Cyclic Voltammetry
DI	Deionized
DLP	Digital Light Processing
DNA	Deoxyribonucleic acid
ECDM	Electrochemical Discharge Machining
ECM	Extracellular Matrix
FDA	Food and Drug Administration
Fe	Iron
FDM	Fused Deposition Modelling
GelMA	Gelatin Methacryloyl
GMI	Giant Magnetoimpedance
GMR	Giant Magnetoresistance
g	Gravitational acceleration vector
HAC	Hybrid Atomistic-Continuum
HDD	Hard Disk Devices
HF	Hydrofluoric Acid
Hz	Hertz
IPA	Isopropyl Alcohol
kg	kilograms
kDa	Kilodalton
L	Liter
LAP	Lithium Phenyl-2,4,6-trimethylbenzoylphosphinate
LoC	lab on a chip

m	metre
mmol	millimole
mV	millivolts
MA6	Mask Aligner Model MA6
MA	Methacrylic Anhydride
MEMS	Micro-Electro-Mechanical Systems
MDEs	Magnetic DNA-encoded probes
MNPs	Magnetic Nanoparticles
Mn	Manganese
MRAM	Magnetoresistive Random Access Memory
ML	Machine Learning
Mw	Molecular weight
nm	nanometre
nT/mA	Nanotesla/ milliampere
Ni	Nickel
pT	Pico Tesla
PASP	Poly (aspartic acid)
PBS	Phosphate Buffered Saline
PCR	Polymerase chain reaction
PCL	Polycaprolactone
PDMS	Polydimethylsiloxane
PEB	Post-exposure bake
PEG	Polyethylene Glycol
PEGDA	Polyethylene Glycol Diacrylate
PGA	Poly glycolic Acid
PGMA	Propylene glycol methyl ether acetate
PLA	Poly lactic Acid
PLGA	Poly lactic Acid-co-glycolic Acid
PLP	Padlock Probe
PM	Particulate Matter
PMMA	Polymethyl Methacrylate
POC	Point-of-Care
POCT	Point-of-Care Testing
PVA	Poly (vinyl alcohol)
RCA	Rolling Circle Amplification
RGD	Arginine-Glycine-Aspartic Acid
RIE	Reactive ion etching
RNA	Ribonucleic acid
rRNA	Ribosomal RNA
RO	Reverse Osmosis
s	second
SAM	Self-assembled monolayer
SF	Silk Fibroin
ST	Salmonella Typhimurium
SU-8	Epoxy-based negative photoresist
SLA	Stereolithography
SQUID	Superconducting Quantum Interference Devices
SWV	Square Wave Voltammetry
TMR	Tunnelling Magnetoresistance

t	Time
UAV	Unmanned Aerial Vehicle
UV	Ultraviolet
v/v	Volume/Volume
V	Velocity vector
V.P	Vibrio Parahaemolyticus
w/v	Weight/Volume
WE	Working Electrode
ZnO	Zinc Oxide

Chapter 1

1. Introduction

1.1 Motivation

There is a growing need for portable and affordable biosensors that enable early disease detection and home-based diagnostics. These devices allow rapid, accurate, and on-site analysis of biomarkers in accessible body fluids, overcoming limitations of traditional diagnostic tools that are often bulky, costly, and dependent on trained personnel [1-3]. Advances in nanotechnology and biosensing have led to the development of various point-of-care systems, including electrochemical, optical, and Deoxyribonucleic acid (DNA)-based biosensors, offering high sensitivity and fast response times [4-6]. Among these, microfluidic biosensors have emerged as especially promising due to their ability to miniaturize biological detection on a single platform. They enable low-volume sample handling, automation, and high-throughput processing [7, 8]. Microfluidic technologies have also opened new possibilities in areas such as antimicrobial resistance testing, cancer diagnostics, and personalized medicine [9, 10]. However, practical barriers such as scalability, device robustness, and seamless integration with digital systems still limit their widespread clinical use [11, 12]. This project is motivated by the opportunity to address these challenges through the development of a simple, cost-effective, and biodegradable microfluidic platform for biosensing applications.

1.2 Goal of the Project

The goal of this project is to develop a biodegradable microfluidic platform integrated with a tunnelling magnetoresistance (TMR) sensor for the detection of magnetic nanoparticles (MNPs) as model targets. The platform is designed to provide a low-cost, environmentally friendly, and portable solution for biomedical diagnostic applications. To support sustainability and biocompatibility, the device is fabricated using biodegradable hydrogel materials such as Polyethylene Glycol Diacrylate (PEGDA) and Gelatin Methacryloyl (GelMA). In addition to using digital light processing (DLP) Three-dimensional (3D) printing for high-resolution microfluidic fabrication, conventional microfabrication methods involving photolithography and Polydimethylsiloxane (PDMS) were also explored. This comparison enables evaluation of practicality, resolution, and material performance across different fabrication strategies. This project aims to address the technical challenges associated with integrating magnetic sensing with microfluidic platforms. The ultimate

objective is to contribute to the development of compact, sensitive, and user-friendly biosensing systems for early disease detection.

1.3 Background on Microfluidics

Microfluidics is a multidisciplinary technology that involves the manipulation of fluids at the microscale, enabling precise control overflow behaviour, mixing, and reaction environments. In biomedical applications, microfluidic systems offer numerous advantages such as low reagent consumption, rapid analysis, and the potential for high-throughput diagnostics [13]. These characteristics make microfluidics particularly suitable for point-of-care biosensing platforms, where compact, sensitive, and cost-effective devices are required [14].

To develop functional microfluidic devices, material selection and fabrication methods are critical. In this project, two photocurable hydrogels PEGDA and GelMA were used due to their biocompatibility, tunable mechanical properties, and biodegradability [15, 16]. PEGDA offers chemical stability and ease of photopolymerization, while GelMA provides a biologically favorable matrix derived from natural gelatin, often used in applications requiring cell interaction and tissue mimicry [17]. For the fabrication of microfluidic channels, both digital light processing (DLP) 3D printing and photolithography were employed. DLP printing is a layer-by-layer photopolymerization method that enables rapid prototyping of high-resolution microstructures, making it ideal for soft, transparent hydrogel materials like PEGDA [18]. In this study, PEGDA formulations were optimized using a Cellink Lumen X printer to achieve precise channel structures with controlled thickness and curing depth. To benchmark performance, photolithography with SU-8 photoresist and PDMS molding was used an established method for fabricating well-defined microchannel networks [19]

According to our target in this study, integration with sensing technology adds a functional layer to the microfluidic platform. This project employs a TMR sensor to detect MNPs as model targets. Magnetic biosensors offer label-free detection, excellent sensitivity, and robustness in complex samples, as they are largely unaffected by optical noise or background fluorescence [20, 21]. The ability to detect varying MNP concentrations within microchannels supports the development of sensitive diagnostic tools that can operate in miniaturized mediums.

Eventually, the combination of biodegradable hydrogels, advanced microfabrication techniques, and magnetic biosensing presents a promising approach for building next-generation biomedical diagnostic devices.

1.4 Scope of the Thesis

This thesis focuses on the design and fabrication of a biodegradable microfluidic platform integrated with a TMR sensor for detecting MNPs as model diagnostic targets. The research involves the synthesis of biocompatible hydrogels PEGDA and GelMA and their application in fabricating microfluidic structures using digital light processing (DLP) 3D printing. To compare the fabrication process, conventional photolithography and PDMS melding techniques were also employed.

The scope of this work includes material preparation, microfabrication process optimization, and experimental evaluation of the microfluidic device's sensing performance using magnetic nanoparticles under controlled conditions. Emphasis is placed on exploring the resolution, structural integrity, and functional performance of the fabricated platforms, particularly their compatibility with TMR magnetic sensors.

This thesis does not aim to detect real biological biomarkers or perform clinical validation. Instead, it focuses on developing a proof-of-concept platform using model particles to evaluate the integration potential of magnetic sensors with biodegradable microfluidics. The work is situated within the broader context of biomedical diagnostics, with potential implications for future point-of-care and environmentally sustainable sensor development.

1.5 Aim and Objectives

The aim of this thesis is to design and fabricate a biodegradable microfluidic platform integrated with a TMR sensor for the detection of MNPs as model diagnostic targets. To achieve this aim, several key objectives were pursued. First, biocompatible and photocurable hydrogels, specifically PEGDA and GelMA, were synthesized and optimized for microfluidic fabrication. The fabrication of microfluidic structures was then carried out using digital light processing (DLP) 3D printing, with adjustments made to printing parameters to improve structural integrity and resolution. In parallel, conventional microfabrication using photolithography and PDMS melding was employed to allow for comparative analysis of fabrication techniques. The integration of a TMR magnetic sensor into the microfluidic platform was subsequently performed to enable magnetic nanoparticle detection. Finally, the sensing performance of the complete system was evaluated by analysing the electrical response of the sensor to various MNP concentrations, thereby assessing the feasibility and sensitivity of the proposed biosensing platform.

1.6 Thesis Outline

This thesis is organized into five chapters. Chapter 1 introduces the motivation, goals, background, and scope of the project, outlining the significance of biodegradable microfluidic platforms integrated with magnetic sensing technology. Chapter 2 provides a comprehensive review of the relevant literature, including microfluidic device design, hydrogel materials, fabrication methods, and magnetic biosensing principles. Chapter 3 details the materials and methods used throughout the project, covering hydrogel synthesis, device fabrication using DLP and photolithography, and the integration and testing of the TMR sensor. Chapter 4 presents the experimental results and discusses the performance of the fabricated platform, focusing on the effectiveness of fabrication techniques and the sensing capability of the integrated system. Finally, Chapter 5 concludes the thesis by summarizing key findings, discussing the limitations of the current work, and suggesting directions for future research.

Chapter 2

2. Literature Review

2.1 Microfluidic

Microfluidics, a multidisciplinary field at the intersection of engineering, biology, chemistry, and physics, focuses on the study and manipulation of fluid flow at the microscale, typically within channels measuring microns in size. This discipline, rooted in fluid mechanics, enables the precise control and handling of extremely small fluid volumes (ranging from approximately 10^{-18} to 10^{-6} litters) through the design and fabrication of microreactors, microchannels, and other miniature systems. Microfluidic platforms typically consist of interconnected components such as channels, valves, chambers, and pumps, allowing the execution of complex biological and chemical processes with high efficiency and parallelisation [22]. The importance of microfluidic systems lies in their ability to perform advanced biochemical analyses with remarkable sensitivity, speed, and portability, effectively overcoming many limitations of traditional laboratory techniques. These systems offer numerous advantages, including reduced power and time requirements, lower sample and reagent consumption, minimal manufacturing and handling costs, and enhanced flexibility and precision in liquid manipulation. As a result, microfluidic technology has gained significant attention for its transformative applications in biomedical research, clinical diagnostics, and analytical chemistry [23-25]. Microfluidics contributes significantly to the development of lab-on-a-chip (LoC) systems, organ-on-a-chip platforms, and biosensors.

The evolution of microfluidic systems is grounded in innovations across electronics, chemistry, and materials science. While early developments in semiconductor technologies such as photolithography and silicon etching were foundational, the field began to take shape in the 1990s with the emergence of micro total analysis systems (μTAS) that integrated lab functions onto a chip [26, 27]. This progress was further accelerated by advances in 3D printing, capillary electrophoresis, and soft lithography, which enabled the miniaturization and automation of biochemical assays [28, 29].

Microfluidic applications have since expanded into point-of-care diagnostics, organ-on-a-chip platforms, and paper-based systems for low-resource settings [30]. Notably, during the Coronavirus disease 2019(COVID-19) pandemic, microfluidics enabled the development of rapid diagnostic devices and rapid screening tools [31-33]. These achievements underline the field's adaptability and relevance to modern healthcare challenges.
To fully harness the potential of microfluidics for biosensing applications, it is essential to

understand the fundamental physical principles governing fluid behaviour at the microscale, which are discussed in the following section.

2.1.1. Fundamental Principles of Microfluidics

Microfluidic systems are governed by the fundamental principles of fluid dynamics, enabling the precise manipulation of fluids at the microscale. These principles underpin core functionalities such as fluid mixing, separation, droplet generation, and particle manipulation, which are essential for diverse applications ranging from diagnostics to drug delivery [34-36]. The behaviour of fluids in microchannels is influenced by parameters such as flow rate, pressure, viscosity, and channel geometry. Consequently, a rigorous understanding of microscale fluid mechanics is vital for the rational design and optimization of microfluidic devices.

At the microscale, fluid flow deviates significantly from macroscopic behaviour. Research conducted at the University of Pennsylvania in the 1990s revealed unconventional flow phenomena that challenge traditional continuum mechanics assumptions [37]. For instance, liquids may exhibit granular-like behaviour, while gases can become rarefied due to the low Knudsen number, and the influence of boundary interactions becomes increasingly pronounced. Such deviations necessitate modifications to classical models like the Navier–Stokes equations:[14]

$$\rho \frac{DV}{DT} = -\nabla p + \rho g + \mu \nabla^2 V$$

where ρ= Fluid density (kg/m³), V is the velocity vector, p is the pressure, g denotes the gravitational acceleration vector, and μ is the dynamic viscosity of the fluid. The term $\frac{DV}{DT}$ is accounts for the fluid's acceleration.

To address these complexities, hybrid atomistic-continuum (HAC) approaches are often employed. These combine molecular dynamics with continuum models to capture microscale effects more accurately. Phenomena such as electrokinetic flows, anomalous diffusion, and thermal creep further complicate system dynamics. Localized computational models that discretize the fluid domain into control volumes are typically used for accurate force estimation and prediction of system behaviour. A key analytical framework in microfluidics involves the use of dimensionless numbers to characterize flow regimes and dominant physical effects. The Re number, defined as the ratio of inertial to viscous forces, is especially significant in determining whether flow is laminar or turbulent. In microfluidic systems, the Re number is typically much less than unity. This indicates that viscous forces

dominate, and flows are predominantly laminar, allowing for precise control and predictable behaviour.

Interfacial phenomena are essential to microscale fluid manipulation. Surface tension and wettability, for example, are fundamental in controlling droplet formation, spreading, and transport. These are key mechanisms in droplet microfluidics and digital microreactors [38, 39]. Surface properties can be engineered through chemical modification or by altering surface roughness, which modulates contact angle hysteresis, flow resistance, and mixing efficiency [40, 41]. Electrokinetic effects, particularly electroosmosis and electrophoresis, are widely utilized to drive fluid flow and manipulate particles without the need for mechanical components. Electroosmosis involves the movement of the entire fluid volume under an applied electric field, whereas electrophoresis refers to the migration of charged species. These mechanisms are critical in electrochemical sensing, separation of biomolecules, and enhancing the sensitivity and specificity of microfluidic biosensors [42, 43]. In addition to interfacial and electrokinetic phenomena, adhesion and cohesion forces significantly influence microscale fluid behaviour. Adhesion describes the interaction between liquid molecules and solid surfaces, impacting wetting behaviour and fluid mobility along channel walls. Cohesion refers to the intermolecular attractions within the fluid, which govern the stability and morphology of droplets, bubbles, and interfaces. These parameters are crucial to emulsion formation, encapsulation, and droplet-based assays [44, 45].

Transport phenomena such as convection, diffusion, and electrophoresis further regulate the movement of fluids, solutes, and thermal energy within microfluidic environments. Pressure or temperature induced convection is commonly employed to guide particle motion, regulate flow direction, or induce mixing, particularly in systems equipped with microheaters or electric field modulators. Diffusion, as a passive transport mechanism, facilitates solute mixing and homogenization, which is particularly relevant in chemical synthesis and controlled drug release systems [46, 47]. Additionally, thermophoresis and electrothermal flows extend control capabilities by exploiting temperature gradients and localized electric fields. Collectively, these principles form the foundation of microfluidic technology. They enable the engineering of compact, multifunctional systems for precise, efficient, and scalable fluid manipulation at the microscale.

Based on these fundamental principles, the design of a microfluidic platform must carefully balance structural, fluidic, and material considerations to achieve reliable and application specific performance. These aspects are examined in the next section.

2.1.2. Design considerations

Design considerations are critical to the successful development of microfluidic devices and must be rigorously evaluated to ensure optimal performance, operational reliability, and compatibility with specific application requirements. These considerations span multiple domains, including structural configuration, channel geometry, fluid dynamics, surface properties, system integration, fabrication methodologies, and biological compatibility, as shown in Figure 2-1 (a, b). Each factor influences the efficiency and functionality of a microfluidic platform under defined operating conditions.

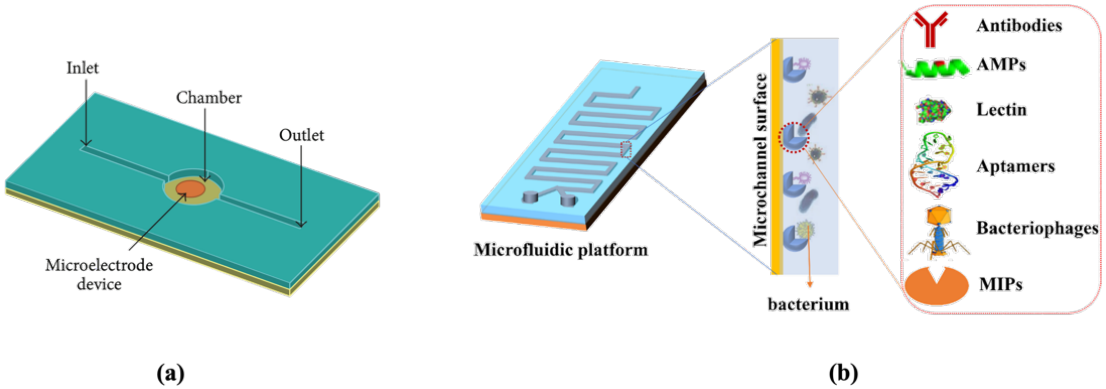

Figure 2-1 (a) Structural configuration and integration of a microelectrode device within a microfluidic platform Adapted from ref. [48], © 2014 Wan Shi Low et al. [CC BY 3.0]. (b) Surface functionalization of microchannels using various biorecognition elements for specific detection. Reproduced with permission from [49], © 2022, Springer-Verlag GmbH Germany, part of Springer Nature.

The overall device architecture should be engineered to minimize dead volumes, maximize the surface area to volume ratio, and promote efficient mixing and fluid transport. Channel geometries such as circular, rectangular, or serpentine profiles are selected based on the intended flow dynamics and the degree of mixing or dispersion required. These design choices must also account for the nature of the working fluid, sample volume, and the specific fabrication process employed. Also, channel layout and dimensions are especially critical in governing microscale fluid behaviour. The width, height, and length of microchannels directly influence parameters such as laminar flow characteristics, diffusion rates, and pressure drops. To enhance passive mixing, microscale features such as grooves, posts, or zigzag structures can be integrated within the channels. These elements disrupt flow symmetry and are particularly effective in low Re number regimes, which are typical in microfluidic systems. Furthermore, the channel architecture must allow for accurate control of flow direction and velocity, which is essential for applications involving sorting, trapping, or compartmentalization of fluids and particles [14].

Furthermore, fluid behaviour can also be modulated by external fields, such as electric or magnetic forces, enabling advanced functionalities through electrokinetic or

magnetophoretic manipulation. Mechanisms like electrophoresis and electroosmosis facilitate particle transport and separation without mechanical components. In parallel, surface properties of the microchannels significantly impact fluid dynamics. Hydrophilic or hydrophobic coatings, as well as functionalized layers such as self-assembled monolayers (SAMs), can be employed to control wettability, reduce nonspecific adsorption, and improve sample retention or separation. These surface treatments are particularly vital in droplet microfluidics and biosensing platforms requiring high sensitivity and specificity [14].

System-level integration is another cornerstone of microfluidic design. Devices must interface seamlessly with auxiliary systems, including micro-pumps, valves, sensors, actuators, and detectors. This is particularly important in LOC applications, where the automation of complex workflows depends on the synchronized operation of fluidic and electronic subsystems. Effective integration ensures minimal user intervention, reliable sample handling, and stable long-term operation. Recent advances have led to the emergence of modular microfluidic platforms that feature standardized, interchangeable components. These modular systems support rapid prototyping, scalability, and multifunctionality, enhancing their utility in both clinical diagnostics and analytical research.

Fabrication techniques exert a significant influence on design feasibility and system performance. Traditional microfabrication methods such as photolithography and soft lithography remain widely used, particularly to produce PDMS-based devices. Soft lithography offers rapid and cost-effective prototyping with high geometric complexity. However, inherent limitations of PDMS, such as poor solvent resistance and high gas permeability, have motivated the adoption of alternative materials and methods. Thermoplastics, including Polymethyl Methacrylate (PMMA) and cyclic olefin copolymer (COC), offer improved mechanical strength, chemical stability, and suitability for mass production.

In the recent years, additive manufacturing techniques, particularly 3D printing, have recently transformed microfluidic fabrication by enabling the creation of complex, multilayered structures with customizable architectures. Technologies such as Stereolithography (SLA) and fused deposition modelling (FDM) allow for the incorporation of multiple materials and embedded components within a single manufacturing process. Additionally, laser micromachining enables high-precision fabrication without the need for photomasks, allowing for rapid design iteration and multilayer device assembly.

Finally, material compatibility with biological specimens is essential for microfluidic systems intended for biomedical applications. Materials must exhibit biocompatibility,

chemical inertness, and non-toxicity to ensure the integrity of cells, proteins, and nucleic acids within the device. While PDMS remains widely used due to its optical transparency and elasticity, its hydrophobic nature and absorption of small molecules can compromise assay performance. Alternative materials such as hydrogels, surface-modified thermoplastics, and biodegradable polymers are increasingly employed to create controlled microenvironments that support sensitive and reproducible biological interactions [14].

A significant element underpinning microfluidic design is the choice of material, which directly impacts biocompatibility, fabrication feasibility, mechanical stability, and compatibility with sensing elements. The next section provides an in-depth review of materials commonly used in microfluidic systems and their relevance to this project.

2.2. Materials

The successful performance of microfluidic devices is strongly based on the selection of materials appropriate for their manufacture. These materials not only facilitate the precise construction of microchannels, but also critically influence the interaction of fluids in the device. Among the most notable materials used in microfluidic manufacturing are glass and polymers, each with distinct properties that contribute to the functionality and efficiency of microfluidic systems. Glass, known for its excellent optical clarity, chemical resistance and thermal stability, is a traditional choice for high precision applications where fidelity and robustness are essential [50]. Its ability to be thermally linked makes it possible to create robust joints, making glass an ideal substrate for organic applications. However, the rigidity and fragility of the glass can make challenges during manufacturing and manipulation. A wide range of materials have been employed in microfluidic fabrication, with glass and polymers being the most used. Glass offers excellent optical clarity, chemical resistance, and thermal stability, making it suitable for high-precision applications [50-52]. However, due to its rigidity, fragility, and higher manufacturing cost, it was not selected for this project. Polymers have emerged as a more versatile and accessible alternative for microfluidic applications.

PDMS is one of the most widely used polymers due to its optical transparency, gas permeability, and compatibility with soft lithography techniques [53]. PMMA is another commonly used polymer offering mechanical strength and chemical resistance, and it supports rapid prototyping through laser cutting [54, 55]. However, the limitations of these polymers such as PDMS's hydrophobicity and poor chemical resistance make them less ideal for certain sensing applications, particularly those involving organic solvents or high precision biosensing. Beyond conventional materials, several natural and synthetic

biodegradable polymers have been explored in recent research. While not used in this project, materials like silk fibroin (SF), chitosan, and polyaspartic acid (PASP) demonstrate the breadth of innovation in the field, supporting applications such as tissue engineering, drug delivery, and environmentally responsive systems [56-58]. These examples, while valuable, are presented for context and are not central to the current work. The insights gained from evaluating different classes of materials laid the foundation for selecting fabrication techniques that align with the structural and processing requirements of microfluidic devices. The following section discusses the rationale behind the chosen fabrication methods and the practical considerations that guided their implementation.

2.2.1. Biodegradable Polymers: Overview and Applications in Microfluidics

Biodegradable polymers are integral to the development of advanced microfluidic systems, particularly for biomedical applications. These materials naturally degrade into by-products such as water, carbon dioxide, biomass, and inorganic salts, making them suitable for transient, implantable, or environmentally friendly applications. Their compatibility with biological surfaces, tunable mechanical properties, and functional chemical structures make them versatile candidates for microfluidic device fabrication [59, 60].

Moreover, PDMS (Polydimethylsiloxane) was also utilized in this study during the preliminary fabrication phase using soft lithography. This process was carried out to evaluate the practicality, time requirements, and infrastructure needed for microfluidic device fabrication using conventional methods. Although PDMS was not selected as the final material due to its known limitations such as hydrophobicity and poor compatibility with organic solvents this step helped highlight the fabrication challenges associated with cleanroom-dependent techniques and provided a standard for comparing alternative biodegradable materials.

Biodegradable polymers are broadly classified into two categories: natural and synthetic. Natural biodegradable polymers, such as polysaccharides (e.g., alginate, chitosan) and proteins (e.g., gelatine, collagen, silk fibroin), are derived from biological sources and are known for their biocompatibility and water-retention capabilities. These materials have been widely used in producing hydrogel-based microfluidics that support 3D cell culture and tissue engineering applications. For instance, alginate and gelatine hydrogels have been employed to fabricate simple, replicable microchannel platforms that mimic extracellular environments, supporting fibroblast and endothelial cell growth [56, 61]. However,

challenges in controlling degradation rate, immunogenicity, and mechanical strength persist in natural polymers.

Synthetic biodegradable polymers, on the other hand, provide greater structural uniformity, controllable degradation rates, and ease of processing. Notable examples include polylactic acid (PLA), polyglycolic acid (PGA), and their copolymer poly (lactic-co-glycolic acid) (PLGA), all of which are FDA-approved for clinical use [62, 63]. These polymers degrade through hydrolysis of ester bonds and are widely used in scaffolds, sutures, and drug delivery systems. PEGDA (Polyethylene Glycol Diacrylate) is a synthetic, UV-crosslinkable polymer widely used in microfluidic fabrication due to its tunable mechanical properties and high biocompatibility.PEGDA-based resins enable high-resolution stereolithography (SL/DLP) printing designed channels, all while maintaining transparency suitable for cell-culture or sensor alignment [64]. It can be rapidly polymerized through photoinitiated free-radical crosslinking, which is highly advantageous for creating well-defined microchannel structures with precision. PEGDA's hydrophilic nature minimizes nonspecific protein adsorption and facilitates smooth fluid flow within the device[65]. Its mechanical stiffness can be adjusted by altering the molecular weight or concentration, enabling custom design for different applications [66]. Importantly, PEGDA is optically transparent, allowing for easy integration with optical and magnetic sensors, including TMR systems. These features make PEGDA a suitable candidate for developing stable and biodegradable microfluidic platforms.

Furthermore, GelMA (Gelatin Methacryloyl) is a semi-synthetic polymer derived from gelatin, functionalized with methacryloyl groups to render it photocrosslinkable. GelMA combines the biological advantages of natural polymers such as cell-adhesive motifs and enzymatic degradability with the structural control provided by synthetic modification. It forms hydrogels that closely mimic the ECM, making it particularly attractive for biomedical microfluidic applications like organ-on-chip and cell encapsulation systems. Although GelMA is softer and more gel-like than PEGDA, its excellent biocompatibility and controllable degradation rates enable applications in dynamic microenvironments. Furthermore, GelMA's Ultraviolet (UV)-crosslinking ability allows precise patterning, which is essential for microscale integration with biosensors and other functional elements [20, 67].

The selection of PEGDA and GelMA in this study was based on their favourable fabrication properties and compatibility with biosensing platforms. While other biodegradable materials have demonstrated success in microfluidics, they were not chosen for this project due to either limited UV crosslink-ability or suboptimal mechanical integration with the TMR

sensor substrate. Understanding the fabrication behaviour and material properties of biodegradable polymers like PEGDA and GelMA informed the development of this study's experimental workflow. These insights contributed to the selection of an appropriate manufacturing strategy, which is outlined in the following section.

2.3 Fabrication

The manufacture of microfluidic devices is a vital component in the realization of their potential and innovation in this sector is essential to satisfy the growing demand for precision tools in health care. Due to the disposable nature of many microfluidic chips, scalable and cost-effective manufacturing is essential [68, 69]. Various fabrication techniques have emerged over time, including chemical, mechanical, laser-based, and additive manufacturing methods. Among these, photolithography and 3D printing have had a particularly transformative impact on the field, allowing for high-resolution fabrication and rapid prototyping, respectively [51].

Conventional manufacturing techniques such as soft lithography, which uses polymer materials such as PDMS, have been decisive to accelerate the development of microfluidic devices [70]. This method is based on the creation of a master's mold that defines the channel geometries, allowing the careful reproduction of microstructures. The advantages of soft lithography include low-cost production, scalability and the ability to create complex 3D structures with a range of surface chemicals. However, these techniques also present limitations, such as the duration of the material and the concerns on biocompatibility, which can hinder long-term applications in medical contexts [71]. Emerging manufacturing techniques are being developed to overcome these limitations and offer additional skills. For example, 3D printing and additive production have emerged as powerful alternatives, allowing customizable projects and quick prototyping. These methods excel in the creation of intricate structures that traditional techniques may not be able to produce. However, the challenges remain in terms of resolution and surface finish necessary for precise microfluidic applications [72]. This thesis emphasises the production of microfluidic devices using photolithography and 3D printing techniques. The following part offers a brief but thorough discussion of the several fabrication methods used in the creation of microfluidic systems.

2.3.1. Chemical Etching Techniques

Concurrently, chemical processes such as wet and dry etching were adapted to produce microchannels in glass and silicon. Wet etching, using chemicals like hydrofluoric acid (HF), enabled simultaneous processing of multiple wafers with high etch rates. However, its

isotropic nature limited feature definition, and the use of corrosive reagents introduced safety and environmental concerns [73, 74].

Dry etching, particularly reactive ion etching (RIE), offered improved control over etch profiles by using directional ion bombardment to create anisotropic structures. This technique became essential for high-aspect-ratio microfeatures, though it was slower and more complex than wet etching [52]. Electrochemical discharge machining (ECDM), introduced later, enabled microfabrication in non-conductive substrates like glass and ceramics by generating localized sparks that eroded material from the surface [75].

2.3.2. Mechanical Micromachining and Xurography

Mechanical methods such as micromilling, ultrasonic machining, and abrasive jet machining were also explored for microfluidic device fabrication. These techniques, derived from traditional machining, offered flexibility and cost-effectiveness for producing master molds or directly patterning substrates [76]. However, their relatively lower resolution and surface finish limited their use in applications requiring precision. Xurography introduces a low-cost, rapid prototyping technique involving computer-controlled cutting of adhesive films using razor blades [77]. This method did not require cleanroom infrastructure and allowed for the rapid creation of simple microfluidic devices, making it suitable for educational purposes and early-stage research [78].

2.3.3. Injection Molding and Hot Embossing

To meet the need for scalable production, injection molding and hot embossing were adapted from conventional polymer processing. Injection molding involved melting thermoplastic pellets and injecting them into a precision-engineered mold under pressure. This method was ideal for high-volume manufacturing but required significant upfront investment in mold fabrication and was limited by the types of thermoplastics that could be used [79, 80]. Hot embossing, on the other hand, pressed a mold into a heated thermoplastic substrate to transfer microstructures. Compared to injection molding, it introduced less residual stress and achieved more accurate pattern replication, though it shared similar material limitations [81]. These methods significantly advanced the commercialization of polymer-based microfluidic devices.

2.3.4. Introduction of Laser-Based Fabrication

Laser-based fabrication emerged as a versatile method for prototyping and customizing microfluidic structures. Laser ablation used focused laser beams to thermally degrade

materials, enabling direct patterning on polymers, glass, and ceramics without masks or chemicals. This method offered design flexibility and rapid turnaround times but was limited by surface roughness, low repeatability, and challenges in achieving uniform depth and feature dimensions [82, 83]. SLA, developed later, used laser or light sources to cure photopolymer resins layer-by-layer. This process enabled the creation of complex 3D structures, including those with internal channels, which were difficult to fabricate using traditional planar techniques. Comina et al. demonstrated that SLA could be effectively used for both direct device fabrication and for mold creation in soft lithography workflows [84].

Photolithography

The earliest microfluidic fabrication techniques were derived from semiconductor processing. Photolithography, a method initially developed for the electronics industry, became foundational for microfluidics due to its precision and compatibility with cleanroom environments. Introduced in the 1960s and widely adopted by the 1980s, photolithography involves transferring a pattern from a photomask to a light-sensitive photoresist on a substrate using UV light. Subsequent development and etching steps create microstructures with sub-micron accuracy [51].

Photolithography provided the resolution and reproducibility required for high-performance microfluidic devices, particularly those fabricated on silicon or glass substrates. However, it demanded cleanroom facilities and expensive equipment, limiting its accessibility to specialized laboratories and industrial settings. The process also lacked flexibility for rapid design changes, posing challenges for prototyping.

In the late 1990s, soft lithography emerged as an alternative that addressed several limitations of traditional photolithography. Introduced by Whitesides and colleagues, this technique involved casting PDMS on a mold fabricated through photolithography, followed by curing and bonding to a substrate [85]. Soft lithography enabled rapid prototyping, design flexibility, and compatibility with biological assays due to the biocompatibility and optical transparency of PDMS [86]. Despite these advantages, soft lithography introduced challenges such as potential pattern distortion during demolding and strong adhesion of cured elastomers to mold surfaces, which could complicate device retrieval [70, 87]. Nonetheless, it represented a paradigm shift by making microfluidic device fabrication more accessible to academic and research laboratories.

2.3.5. 3D-printed microfluidic devices

Recent advancements in 3D printing have revolutionized microfluidic device fabrication, offering advantages over traditional soft lithography techniques. 3D printing enables rapid prototyping, complex 3D architectures, and cost-effective production [88]. Various 3D printing methods, including SLA, fused filament fabrication, and vat polymerization, are being explored for microfluidic applications [89]. These techniques allow for the integration of multiple materials and functionalities within a single device [90]. 3D-printed microfluidics have shown promise in biomedical applications, such as diagnostic chips for disease detection and cell culture studies [91]. However, challenges remain in achieving high resolution, biocompatibility, and optical transparency comparable to traditional methods [92]. As the field progresses, 3D printing is expected to become the dominant fabrication method for microfluidic devices, offering new opportunities for researchers across various disciplines [88]. The following section presents an overview of the various 3D printing techniques (Figure 2-2).

FDM is one of the most accessible 3D printing techniques, using thermoplastic filaments heated at their merger and extruded point through a nozzle. This method is particularly advantageous for the creation of basic microfluidic structures due to its rapid capacity for prototyping and low material costs. However, the intrinsic resolution limits of FDM, generally in the interval from 200 to 500 μm, can limit the purposes necessary for high - performance microfluidic applications [93].

On the contrary, SLA and DLP use photopolymerization techniques, in which a liquid resin is treated by layer for layer by UV light. These methods allow a higher resolution, reaching sub-50 μm characteristics, which is essential for the planned intricate channels projects in applications such as single cell analysis [94]. The ability of SLA and DLP to produce highly precise microstructures expand their applicability in diagnostics and biotechnological fields, in the analysis devices on chips and in organ-on-a-chip models.

DLP is an advanced 3D printing technique that utilize projected light to polymerise photopolymer resins incrementally, offering superior resolution and accuracy [95]. Photosensitive resins are employed in DLP printers, with printing conditions such as orientation and layer thickness influencing the printed component's material properties [96]. Recent developments in DLP include material innovations, including four-dimensional (4D) printing of smart materials, piezoelectric ceramic substances, and recyclable resins [95]. DLP is used throughout several domains, such as microfluidics [97], soft robotics, wearable electronics [98], and biomedical engineering [99]. The method allows for the accurate

fabrication of medical devices, specialized artificial tissues, as well as drug delivery systems [100]. Although DLP offers the benefits of resolution as well as efficiency, challenges in achieving finer features as well as an increased range of materials continue [101]. The future focus is on enhancing precision, large-scale prints, multi-material prints, as well as increasing speed [97].

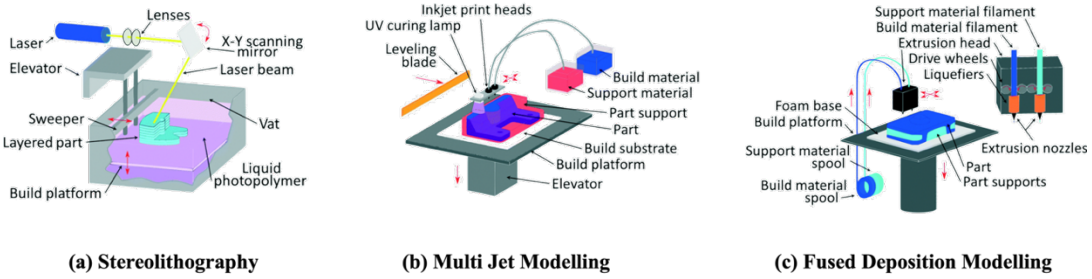

Figure 2-2 Various 3D-printing techniques. (a) SLA; (b)multi jet modelling (MJM); (c) FDM Reproduced from [102], N. Bhattacharjee, A. Urrios, S. Kang and A. Folch, Lab Chip, 2016, 16, 1720 with permission from the Royal Society of Chemistry.

The selection of the material is fundamental in 3D printing, as it directly influences mechanical properties, chemical resistance and the biocompatibility of the resulting microfluidic devices. Various resins, thermoplastic and even hydrogels have been explored for their compatibility with 3D printing techniques, with research that indicates that materials such as PEGDA and PLA are particularly promising due to their favourable properties for biological and mechanical properties [103]. However, while many materials used in 3D printing can offer excellent structural integrity, their interaction with biological champions during diagnostics is a fundamental consideration that can affect performance and accuracy.

Building upon these advancements in material selection and printing resolution, 3D-printed microfluidic devices have since been applied in diverse scientific domains. In developmental biology, Grebenyuk et al. used two-photon polymerisation to fabricate a perfusable microvascular network for large-scale tissue culture and nutrient delivery [104]. Knoška et al. developed customized nozzles and mixers for time-resolved structural biology using X-ray free electron lasers, improving the resolution of dynamic imaging [105]. In cell biology, McLennan et al. fabricated Two-Photon Polymerization (2PP)-printed microfluidic chips to support cell proliferation and delivery of biomolecules [106]. In chemistry, Zhang et al. created a dual-chamber device for real-time monitoring of Pseudomonas aeruginosa biofilms using electrochemical signals, fabricated using SLA-based molds [107]. Wearable applications have expanded rapidly. Nightingale et al. developed a droplet-based sensor integrated with a PDMS microfluidic chip for biomolecule concentration monitoring [108]. Ye et al. created a non-invasive wearable aptamer biosensor, printed via Inkjet Printing, for monitoring estradiol levels in sweat [109]. Li et al. developed fish gill-inspired filtration

membranes for water purification, while Dai et al. used indirect 3D printing to fabricate bionic compound eyes for wide-angle imaging and sensor applications [110, 111].

In this study, a Digital Light Processing (DLP)-based bioprinter was selected due to its ability to achieve high-resolution fabrication while maintaining biocompatibility a critical factor for applications involving biological sensing and biodegradable materials. DLP offers superior spatial precision compared to extrusion-based or FDM printing methods, enabling the creation of microscale channels and features that are essential for controlled fluid dynamics in microfluidic systems. Moreover, the printer's compatibility with UV-crosslinkable biodegradable polymers such as PEGDA made it particularly suitable for this project. While preliminary trials with GelMA were explored, PEGDA was ultimately used due to its more favorable crosslinking behavior and mechanical consistency during printing. The selection of a bioprinter, rather than a conventional DLP printer, also aligns with the project's biomedical focus, as it provides environmental controls (e.g., temperature, sterility) that support future integration with cell-compatible systems. This choice reflects a balance between fabrication precision, material compatibility, and long-term research goals.

Table 2-1 Summary of microfluidic fabrication methods with their advantages, limitations, and materials.

Process	Method	Advantages	Disadvantages	Materials	Ref.
Chemical	Wet Etching	High etch rate can process multiple wafers simultaneously	Requires strong, hazardous chemicals; isotropic etching limits precision	Glass, silicon	[73]
	Dry Etching (Reactive Ion Etching)	Precise, anisotropic patterns; suitable for clear materials	Slower than wet etching; requires specialized equipment	Glass, silicon	[74]
	Electrochemical Discharge Machining	Applicable to non-conductive materials; precise material removal	Limited to specific materials; complex setup	Ceramics, glass	[52]
Mechanical	Micromachining	High dimensional precision, crack-free surfaces	Lower precision and productivity compared to lithography	Silicon, glass, polymers	[76]
	Xurography	Affordable, no clean room required, fast production	Limited precision; not suitable for complex structures	Adhesive films	[112]
	Injection Molding	High efficiency, low cost, precise	Limited to thermoplastics; expensive molds with limited resolution	Thermoplastics	[79]
	Hot Embossing	Less stress and shrinkage than injection molding; high accuracy	Limited to thermoplastics; slower process	Thermoplastics	[81]
	Soft Lithography	High-resolution, low cost, fast, optically transparent, 3D structures	Difficult mold detachment; potential pattern distortion	Elastomers	[82]
Laser-based	Laser Ablation	Fast, flexible, no chemical hazards; suitable for various materials	Low repeatability, adverse surface effects, limited throughput	Polymers, glass, ceramics	[73, 83]
	Stereolithography	Fast prototyping, suitable for sensitive 3D structures	Limited to photopolymers; requires precise laser control	Photopolymers, resins	[84]

3D Printing	Direct Fabrication	Simple process, cost-efficient, flexible; suitable for lab validation	Material limitations: post-processing required	Thermoplastics, photopolymers, elastomers, ceramics	[89]
	Indirect Fabrication (Non-Sacrificial Molds)	Compatible with traditional materials (e.g., PDMS); cost-effective for mass production	Requires bonding step; material compatibility issues	Thermoplastics, photopolymers, elastomers	[113]
	Indirect Fabrication (Sacrificial Molds)	Enables complex channel designs; efficient for mass production	Requires careful material selection; additional purification steps	Thermoplastics, Water soluble polymer, elastomers,	[114, 115]

A thorough understanding of fabrication approaches sets the stage for exploring how these microfluidic platforms are applied in real-world scenarios. The following section introduces key application areas, highlighting the role of microfluidics in fields ranging from diagnostics to environmental monitoring.

2.4. Applications

Microfluidics has been used in several interdisciplinary domains, with numerous applications classified under broad themes like LoC (Figure 2-3) and "Organ-on-a-Chip" [116]. These topics include a variety of applications, such as the manipulation of tiny fluid volumes, the development of microscale ecosystems, and the integration of biological components for research purposes [117]. In this section, was explored the applications of microfluidics in different areas of biosensing research. Microfluidic biosensors are currently widely used across diverse domains, ranging from practical applications to fundamental research. The aim of this section is not to provide an exhaustive list of application fields but rather to highlight the latest advancements and developments in research, particularly as they relate to the use of microfluidic biosensing.

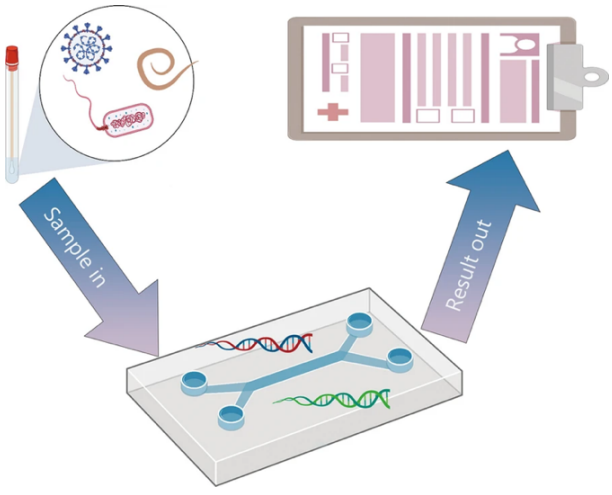

Figure 2-3 Schematic of a LoC system, Reproduced from[118], Xin Wang et al ,Military Medical Research, 2022, licensed under CC BY.

2.4.1. Lab-on-a-chip

LoC devices, or μTASs, are compact platforms that consolidate many laboratory tasks into a single chip or substrate. These devices use microfluidic technology, which entails the manipulation of minute fluid quantities, often in the microlitre or nanolitre range, inside microscale channels inscribed or formed on the chip. LoC systems have attracted significant attention and recognition for their ability to perform many tasks rapidly, efficiently, and with reduced sample and reagent consumption compared to traditional laboratory setups. Portable LoC devices, designed to automate complex diagnostic processes often performed in centralised laboratories, may provide crucial health-related information to healthcare providers and patients in remote locations[119].

The inception of LoC technology dates to the 1960s, when researchers used photolithography techniques to construct micro-electro-mechanical systems (MEMS) [120, 121].

Significant research on LoC began in the late 1980s, after the advent of microfluidics and the use of microfabrication techniques to produce polymer chips. During the 1990s, researchers concentrated on the miniaturisation of biological processes, including Polymerase chain reaction (PCR), using microfluidics, enabling operations on individual cells for the first time. Biochemical techniques, including DNA microarrays [122], electrophoresis [123], PCR [122], and cell lysis, have undergone extensive examination for their miniaturisation, culminating in the integration of all critical processes, from sample collection to final analysis, onto a single chip, thereby demonstrating the full capabilities of LoC technology. In the field of proteomics, LoC facilitates the integration of many phases of protein analysis onto a singular chip [123].

By using these integrated processes, protein analysis may be accelerated from hours with conventional systems to just minutes with LoC devices [124]. In the domain of cell biology, LoC has the ability to govern cells at the single-cell level [125]. For instance, with high-throughput antibodies, one may detect and isolate a particular cancer cell that exhibits fluorescence [126]. These high-throughput methods significantly enhance our ability to isolate and analyses rare cancer cells and specific antibodies, potentially improving cancer diagnostics and therapeutic development. In the realm of molecular biology, LoC technology offers a myriad of options for DNA and RNA sequencing. The Human Genome Project, which took 13 years for completion, might now be accomplished in a few weeks with LoC DNA microarrays. Moreover, nanopore technologies, although being in their nascent phase, elevate genome sequencing to a superior level. These surpass DNA microarrays in speed.

Likewise, LoC has significant promise for immunoassays by decreasing the test duration from around 10 minutes to just seconds [14].

Designing microfluidic LoC devices is intricate and laborious, requiring proficiency in fluid dynamics, mechanical design, and fabrication. Engineers have significant challenges in the development of microfluidic devices owing to a scarcity of specialised instruments that facilitate the process. They are required to do manual investigations of architecture, design device layouts, optimise manufacturing processes, and coordinate valve sequences. Moreover, engineers encounter difficulties in testing and optimising the chip to ensure dependable execution of biological tests [127].

2.4.2. Organ-on-a-chip

Among the most promising and advanced developments to arise from LoC technologies is the creation of organ-on-a-chip devices, which seek to mimic the function of human organs with incredible fidelity. Organ-on-a-chip is an advanced in vitro system that provides a closer simulation of physiological functions of in vivo tissues compared to traditional cell-based models [128]. These technologies simulate multicellular architectures, physicochemical microenvironments, vascular perfusion, and tissue-tissue interactions, achieving higher degrees of organ and tissue function compared to traditional Two-dimensional (2D) and 3D culture methods. Organ-on-a-chip technologies facilitate high-resolution, real-time imaging of live cells within an operating tissue and organ architecture [129]. The primary objective of organ-on-a-chip technology is to generate human tissue models to be used in pharmacological testing and simulation of disease. These systems are able to promote tissue growth, organ function, and disease pathogenesis [130, 131].

These are crucial for the evaluation of molecular modes of action, screening of toxicities, the discovery of biomarkers, and lead candidate selection in the discovery and development of drugs[132, 133]. Organ-on-a-chip devices are expected to develop into sophisticated miniaturized multi-organoid models that integrate human physiology with cellular models, offering enormous potential for the advancement of pharmacologic and disease modelling and the conduct of biomedical studies. Organs-on-chips has enormous potential to explore vital organ function and diseased conditions. Organ-on-chip models of the brain [134], heart [135], eyes [136], muscle [137], lungs [138], liver [139], and other organs have all been developed by researchers.

2.4.3. Environmental Applications

Microfluidic devices proved to be extremely promising in environmental monitoring because of the miniaturized form, portability, sensitivity, and specificity. The small-scale analytical devices are able to analyses very small fluid quantities and are very useful for the detection of trace levels of contaminants in water, air, and soil.

The key benefit of microfluidics in environmental monitoring is its flexibility to detect a wide variety of analytes such as organic and inorganic chemicals, heavy metals, and biological contaminants. Moreover, microfluidic devices are conducive to real-time monitoring, automation, and cost-efficient operation in resource-deprived or inaccessible areas. Typically, techniques include the isolation and pre-concentration of the analytes followed by spectroscopic, chromatographic, or electrochemical detection. Moreover, features of on-site monitoring on an ongoing basis facilitate the detection of the causes of contamination and the effectiveness of mitigation planning.

Microfluidic devices were employed in the assessment of water quality in rivers, lakes, and seas to track contaminants like heavy metals and microbials [140, 141]. A paper disc microfluidic system using upconversion fluorescence and aptamer probes was designed by Jin et al. for on-site screening of water contaminants [142]. A microfluidic bioreactor with replication of the gut-like architecture was proposed by Chen et al. to estimate biochemical oxygen demand. The system uses ambient microbial adhesion to establish an auto-renewal biofilm on the reactor surface, which dynamically adjusts to environmental conditions and allows for biodegradation analysis [143].

Fahimi et al. created a wearable particulate matter (PM|)2.5 sensor using a mass-sensing resonator. The mobile system-compatible device was able to detect particulates at the concentration level of 1 $\mu g/m^3$ within an integration period of 7 minutes at an otherwise noisy environment [144]. Sun and co-workers further built on this by designing a microfluidic chip integrated into an unmanned aerial vehicle (UAV) with colorimetric paper-based sensor for trace metals detection. By using data acquisition through the mobile phone, the system successfully identified Cobalt (Co), Copper (Cu), Iron (Fe), Manganese (Mn), Chromium (Cr), and Nickel (Ni) in air particulate matter within 30 minutes, with the capability to achieve cost-effective and high-density production (48 chips within 30 seconds at $1.92 per unit) [145].

Soil quality assessments have also gained from microfluidic integration, particularly in the agricultural environment. The detection of contaminants including pesticides, organic residues, and heavy metals has been achieved using devices. A paper-based microfluidic

chip that extracts, filters, and concentrates the remnants of explosives from soil samples was presented by Ueland and co-workers. Their system allowed the detection of eight different explosives using fluorescence quenching and provides an effective field-deployable tool for environmental safety monitoring [146]. With ongoing technological advancements, microfluidics is expected to underpin a new generation of point of care (POC) environmental diagnostic tools, empowering communities and researchers to monitor ecological health with enhanced accessibility, accuracy, and responsiveness.

As microfluidic applications expand, their integration with biosensors emerges as an important advancement for developing compact, sensitive, and efficient analytical systems. The next section explores this intersection, focusing on how microfluidics enhances the performance and functionality of biosensors.

2.5. Biosensors

Biosensors are considered as highly promising analytical tools with prospective uses in the fields of drug discovery, medical diagnosis, food safety, and environmental monitoring, and security and defence. The integration of biosensors with microfluidic technology has produced new opportunities for the creation of advanced systems [147]. This section discusses the concepts, the function of microfluidics, and the potential of magnetic biosensors. The biosensors were first published by Leland Charles Clark Jr. in 1962, where they put forward the idea of exhibiting the components of the biosensor along with an approach to combine a bioreceptor with the transducer device [148]. Biosensors are valuable devices employed in academia, the industrial sector, and the research labs [148]. Biosensors in body fluids such as blood, urine, saliva, tears, and sweat sense diseases, contamination of water, and pathogenic microorganisms, and act as biomarkers [149]. Biosensors have opened new horizons within the biological sciences, increasing the benefit to humanity, health care, food safety, and environmental monitoring [150]. They can also aid in high-throughput screening, national defence, food safety, agriculture, medicine, environmental protection, and pharmacology [148].

Biosensors are available in many sizes, forms, and electrode materials, capable of detecting and assessing viruses, infections, and illnesses. They manifest as a compact probe or electronic apparatus that produces an indicator for quantifying subsequent processing; the electronic device facilitates communication, documentation, and detection of alterations in the physiological parameters of biological or chemical constituents in the environment. The apparatus comprises (i) an analyte, (ii) biological material, (iii) a transducer, (iv) an electronic module, and (v) a display unit. Biorecognition generates a signal during the

interaction between the analyte and biological components, while the transducer converts this biorecognition signal into a measurable electrical form, indicating the presence of a biological or chemical target. The interactions between the analyte and bioreceptor correlate with the electrical or optical signals generated by the transducers, which may be linked to a cloud server for data access and storage; the resultant data may be presented as graphical, numerical, or tabular analysis. Biosensors may be categorised into electrochemical, optical, and magnetic varieties based on the transducer used. [148]. Figure 2-4 illustrates the working principle of a biosensor, highlighting the interaction between its components and the signal generation process.

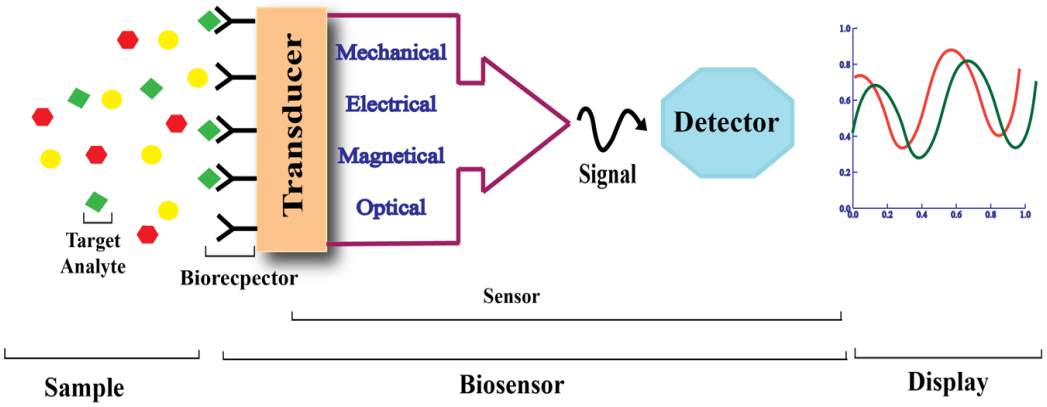

Figure 2-4 principle of a biosensor.

One area of research or work that has benefited greatly from the use of microfluidics is biosensing, where microfluidic chips are integrated into biosensor setups.[117] The integrated microfluidic chip provides the biosensor with the advantage of small analyte volumes, automation, and multiplexity. The use of microfluidic chips will enhance biosensor performance at the point of care by boosting sensitivity, selectivity, and quick detection [151]. Microfluidic chips can be integrated into any kind of biosensor, including optical biosensors, which use the chip to analyse molecular interactions with light in real-time, and microarray biosensors, which use the chip to channel fluids to microwells for molecular analysis, and other types of biosensors that will be covered in later section [152].

2.5.1 Microfluidics in biosensors

Microfluidics provide meticulous regulation of flow rate, sample volume, channel volume, channel height, and response time, hence enhancing the precision and repeatability of findings [153, 154]. Microfluidic chips minimise the diffusion distance between binding molecules, hence decreasing test time and enhancing sensitivity by amplifying molecular interactions [155]. Laminar flow in microfluidic channels disperses analyte molecules extensively and evenly throughout the sensor surface, facilitating more consistent binding

and detection [156]. Microfluidic chips may consolidate several functionalities inside a single device, eliminating the need for supplementary equipment or instruments, hence facilitating streamlined and automated biosensing systems [157]. Microfluidic chips facilitate the automation of biosensing systems by integrating many functionalities, hence enhancing efficiency and minimising the risk of human error [158].

Since the 1990s, microfluidic biosensors have progressed via the miniaturisation of LoC technology [159]. Initial uses included DNA analysis, PCR, and enzymatic reactions [160].During the 2000s, biosensors were incorporated into microfluidic systems, improving sensitivity [161]. Electrochemical biosensors have been prominent for the detection of proteins, nucleic acids, and tiny compounds [162, 163]. By the mid-2000s, POC diagnostics progressed with the development of portable pathogen and biomarker detectors [164]. Advancements in the late 2000s enabled multiplexed assays for genomes and infectious disease diagnostics [165]. High-throughput screening enhanced the efficiency of biological analysis. The 2010s saw the emergence of wearable and implanted biosensors for continuous health monitoring [166-168]. Paper-based microfluidic devices (μPADs) have been developed for low-resource diagnostic applications [169]. The incorporation of AI currently allows real-time biological analysis, enhancing diagnostic precision [170]. The COVID-19 pandemic expedited the implementation of microfluidic biosensors for swift viral detection [171]. Nanomaterials, such as graphene and carbon nanotubes, have improved the sensitivity of biosensors [172].

Gomes et al. devised an electrochemical sensing platform based on bacterial cellulose for POC detection, using the screen-printing technique. The substrate containing bacterial cellulose exhibited significant mechanical property resilience, even when assessed in an aqueous solution. Lactate was quantified in synthetic sweat with a disposable paper-based biosensor and 50 μL of a response sample. The engineered biosensor had an outstanding response in the amperometry approach, identifying lactate concentrations between 1 and 24 mmol L^{-1} in synthetic sweat, with a detection limit of 1.31 mmol L^{-1} and a quantification limit of 4.38 mmol L^{-1}[173].

Jaligam et al. present a cost-effective, microfluidic biosensor featuring three electrodes fabricated via ink-jet printing on a paper substrate, wherein zinc oxide (ZnO) nanoparticles are deposited onto a working electrode (WE) to facilitate the operation of cyclic voltammetry (CV) and square wave voltammetry (SWV). The impact of modifying picric acid concentration and varying scan speeds from 10 to 300 mVs^{-1} was investigated. The experimental linear range was from 4 μM to 60 μM, with a detection limit of 4.04 μM, which is well within the safety threshold of 8 μM [174].

Park et al. examine current advancements in the design of biosensors incorporated into POC devices, emphasising biomolecule detection and intraoral fluid analysis. These advancements possess the potential to substantially improve the functionality and use of biosensors in healthcare environments. Park et al. concentrated on the creation of molecularly imprinted polymers (MIP)-based biosensors incorporated into point-of-care testing (POCT) devices for evaluating intraoral fluids. Their methodology included the synthesis of MIPs exhibiting increased selectivity and chemical affinity for certain biomolecules, hence enhancing diagnostic precision and stability under adverse conditions. In their publication, they emphasise several practical use of MIP-based biosensors, including disposable POC testing devices for monitoring biomarkers in diverse biofluids [175]. The authors examine the prospects of wearable MIP-based biosensors for ongoing health surveillance, especially concerning dental conditions such as periodontitis. Future research priorities include enhancing the selectivity, stability, and scalability of MIP-based biosensors for expanded clinical and environmental applications. A significant constraint identified in the study is a possible problem with mass manufacturing and scalability. This technology facilitates the creation of dependable, non-invasive diagnostic instruments in healthcare [175].

Ma et al. developed a DNA microarray approach enabling pneumonia patients to concurrently identify fifteen distinct bacterial species from their respiratory tract; the test targeted 16S rRNA genes and other specific genes of each pathogen, with a detection limit of 103 copies/μL[176]. A simple microfluidic apparatus including six parallel channels was designed and fabricated using flow-through reaction cells. Photonic crystal beads were introduced and confined inside a metallic microchannel array [177]. The sample interacts with probe molecules immobilised on the surface of the photonic crystal bead array as it traverses the metal microchannels [178]. Microfluidic technology may enhance exposure by transporting samples via microarrays. Furthermore, the fabrication of new low-density and high-density arrays represents a significant use of microfluidic chips [179]. The multiplex test findings are shown, including an epifluorescence picture and an epi-white light image obtained from the base of the reaction cell, serving as the detection and encoding images, respectively.

Additionally, combining advanced materials like nanoparticles and surfaces designed at the nanoscale is another important improvement in microfluidic biosensor technology. Recent studies [119] show that changing the sensor surfaces with nanomaterials improves the parts of the biosensors, making the detection more sensitive and specific. This enhancement is essential because detection of low-abundance biomarkers is needed in applications such as

the early diagnosis of diseases and the surveillance of therapy. The miniaturisation trend enhances the biosensing process and makes the integration of the multiplexed detection capabilities, enabling simultaneous analysis of various biomarkers within one assay.

Furthermore, the future of microfluidic biosensors in health diagnostics is anticipated to be shaped by advancements in materials science, nanotechnology, and artificial intelligence. The advancement of biocompatible nanomaterials, including graphene and gold nanoparticles, is expected to enhance the capabilities of microfluidic devices, facilitating the invention of innovative biosensors that bridge the gap between laboratory environments and therapeutic settings [180]. The integration of artificial intelligence algorithms and automatic learning in microfluidic platforms offers interesting perspectives for real-time monitoring and data analysis, thus improving the decision-making process in clinical practices. Therefore, the continuous evolution of microfluidic technologies has great potential to face pressing health challenges and advance research applications in different sectors., Technological progress in microfluidic has considerably improved the sensitivity and specificity of biosensors, thus transforming their applicability in health diagnostics. A notable trend is the incorporation of artificial intelligence (AI) and machine learning (ML) in biosensors technologies, which facilitates the interpretation of complex data sets generated during Biosensor tests. Recent studies, such as those carried out by Noor et al. [181], have demonstrated how AI algorithms can improve the accuracy of cancer screening by identifying and analysing complex models in biological data, which would be difficult for traditional diagnostic methods. The fusion of AI with microfluidic systems rationalizes the diagnostic process, allowing rapid and precise identification of critical biomarkers for early detection of diseases.

Generally, the reviewed literature on microfluidics in biosensors highlights essential requirements such as high sensitivity, reduced sample volume, and automation. These factors informed the use of PEGDA as a material due to its optical clarity and smooth fluid handling and justified the use of high-resolution 3D printing for microchannel fabrication.

2.5.2. Magnetic biosensors

Magnetic biosensors have become prominent in biomedical applications for their sensitivity and specificity. It is noted by Gungun Lin et al. [182] that magnetic sensing technologies, and specifically magnetoresistive sensors, offer compact integration and less susceptibility to intricate biological samples. Magnetic biosensors use magnetic nanoparticles and microparticles measuring 5–300 nm and 300–500 nm, respectively, inside microfluidic channels, using the magnetoresistance effect. [149, 183]. The surfaces of these particles are altered and functionalised to selectively identify certain compounds with notable sensitivity.

Magnetic biosensors have garnered the interest of researchers due to their significant benefits over fluorescent-based techniques. Magnetic probes exhibit greater stability over time in culture and may be used for prolonged labelling tests without inducing background noise effects. Magnetic fields on exterior surfaces provide remote assessment and control of the biological environment. Furthermore, their potential great sensitivity enables detection at far lower protein concentrations than fluorescent-based methods.[184]. Magnetic microfluidic chips use magnetic fields and particles to modify and detect analytes. They are beneficial for applications including Microfluidic chips for DNA analysis provide benefits including diminished sample and reagent quantities, expedited analysis, elevated throughput, and mobility. They are essential in biosensor research because of their sensitivity and selectivity. Hatamie et al.; Hernandez-Vargas et al. The use of carbon nanomaterials, magnetic microbeads, noble metal nanoparticles, and quantum dots into electrochemical sensors enhances DNA sensing efficacy. Electrochemical biosensors identify interactions between analytes and biological recognition elements, using diverse recognition layers, such as nucleic acid probes or antibodies, and employing detection methods, including colorimetric, optical, and electrochemical approaches [185, 186].

Hernandez-Neuta et al. created a microfluidic magnetic fluidised bed for high-throughput DNA analysis inside a continuous flow system. They optimised a cost-effective polymer microarray for single molecule digital read-out with padlock probes and rolling circle amplification [187]. The device included a rhombic microchamber containing magnetic beads and a permanent magnet, generating a magnetic field gradient that enhanced hybridisation and mixing. The expansive rhombic chamber housed the microarray, facilitating modular solid-phase transfer operations such as DNA capture, padlock probe (PLP) ligation, rolling circle amplification (RCA), and restriction digestion. The flat microarray surface enabled the direct detection and measurement of rolling circle products at low concentrations.

Microfluidic biosensors transform cell-based research by enabling precise flow regulation and cell manipulation. Microvalves and micropumps regulate fluid flow, facilitating operations such as cell sorting, sample loading, and mixing for precise analysis. Microstructures like micropillars provide spatial regulation for cell entrapment, immobilisation, and release, allowing for meticulous manipulation in investigations of cellular behaviour, cell–cell interactions, and pharmacological screening. Methods such as hydrodynamic focussing, dielectrophoretic, acoustic trapping, and magnetic manipulation augment cellular control [188].

Yu, J. et al. (Figure 2-5) created an innovative dual mode aptasensor designed to provide a sensitive and on-site approach for the concurrent detection and quantification of diverse harmful bacteria in food. This advanced aptasensor integrates colorimetry with a microfluidic chip for the swift screening and accurate quantification of bacteria such as Salmonella Typhimurium (S.T) and Vibrio Parahaemolyticus (V.P). It enables the visual identification of infections by the unaided eye, accompanied by concurrent quantification via the microfluidic chip. Magnetic DNA-encoded probes (MDEs) using rolling circle amplification of DNA facilitate a colour development scheme. EcoRV endonuclease may cleave these probes to generate DNA fragments, which are then sorted and measured by the chip. The aptasensor visibly detects 100 Colony-Forming Unit (CFU)/mL of S.T or V.P, and as low as 32 CFU/mL of S.T and 30 CFU/mL of V.P utilising the chip, during a duration of 3 minutes. The device has excellent sensitivity, with a detection limit of 30 CFU/mL, and combines colorimetric techniques with microfluidic chips for prompt, on-site, and dependable identification of foodborne bacteria. [188].

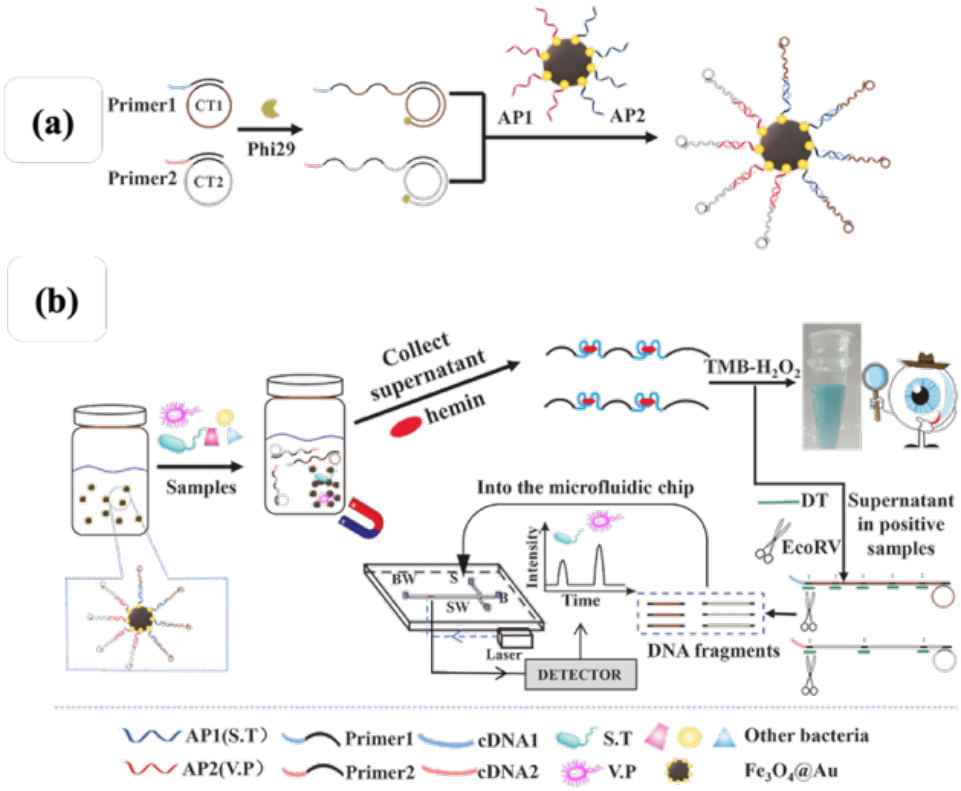

Figure 2-5 (a)The production of MDEs and (b)the dual mode aptasensor for assessing the presence and simultaneous quantification of S.T. and V.P. Reprinted from ref. [188], Jiale Yu et al. Talanta, Vol. 225, 2021, p. 122062, with permission from Elsevier.

Doostmohammadi et al. (Figure 2-6) provide a novel method using Cell-Imprinted Polymer (CIP)-coated microparticles inside a magnetophoretic microfluidic system for the detection of luminous bacteria in water. This technique represents a significant advancement in environmental monitoring and public health by facilitating rapid and precise identification

of bacterial pollutants. Doostmohammadi et al. indicated that their microfluidic device is capable of detecting biomarkers at very low concentrations, making it appropriate for early illness identification. The enhanced microfluidic architecture augmented fluid management and sensor reaction time, crucial for real-time diagnostics. The work [189] presents an innovative technique for the rapid and economical identification of bacteria in water using CIP-Microparticles (MPs) incorporated into a magnetophoretic microfluidic apparatus. This method seeks to fulfil the need for effective point-of-need bacterial detection, especially for pathogens such as Escherichia coli (E. coli), which present considerable health hazards via contaminated water and food sources. The research used fluorescent magnetic CIP-MPs for the collection and detection of microorganisms. The microfluidic device used soft ferromagnetic microstructures to augment the accumulation of CIP-MPs inside the microchannel, optimising the magnetic field distribution for efficient bacterial capture [189].

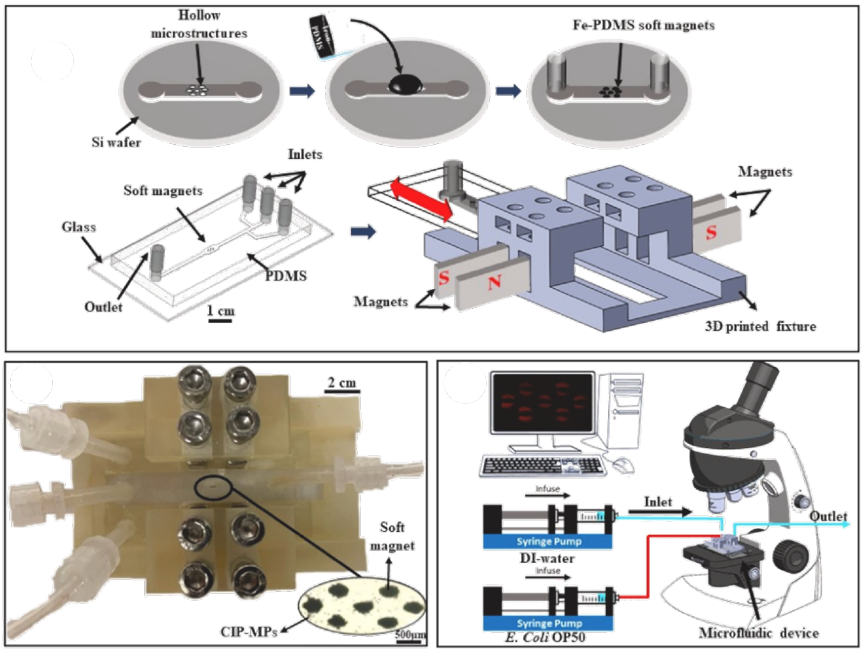

Figure 2-6 Fabrication process of the microfluidic device and experimental configuration. Reprinted from ref. [189] Doostmohammadi et al.Talanta, Vol. 268, 2024, p. 125290, with permission from Elsevier.

The development of magnetic sensors has been a human endeavour for ages. The primary motivation for this, for an extended period, was the detection of the geomagnetic field for navigational purposes. This resulted in the creation of the magnetic compass, after which humanity was no longer dependent on the stars for navigation across perilous seas. This singular innovation precipitated a significant era of expansion, affluence, and advancement. This sensor's adaptability and enduring relevance are shown by its continued existence today as miniaturised solid-state magnetic sensors, alongside several other sensors [190, 191].

Magnetic sensors have been developed utilizing various physical phenomena such as Electromagnetic Induction, Hall Effect, TMR, giant magnetoresistance (GMR), Anisotropic

Magnetoresistance (AMR), and Giant Magnetoimpedance (GMI) [192]. For applications requiring the utmost sensitivity, superconducting quantum interference devices (SQUID) are the preferred option[193]. Solid-state Hall effect, GMR, TMR, AMR, and GMI sensors are produced by planar microfabrication techniques and provide great sensitivity within a small form factor. The compatibility of solid-state magnetic sensors with complementary metal-oxide-semiconductor (CMOS) fabrication processes enables the simultaneous integration of sensors with sensing and computing circuitry, resulting in systems on chip that are highly desirable for Internet of Things applications [194].

Georgios Kokkinis et al. developed an automated microfluidics channel for the separation and counting of cancer cells by using integrated GMR sensors and functionalised magnetic particles (MPs) as shown in Figure 2-7. The method employs magnetic manipulation and conducting microstructures to enable the tagging and isolation of cancer cells. Different reactions to magnetic fields without fluid movement provide a distinct separation concept separating magnetically marked cells from loose MPs. The platform also uses a tapered conductor to line magnetic particles in a linear pattern, therefore enabling successive detection by the GMR sensor [195].

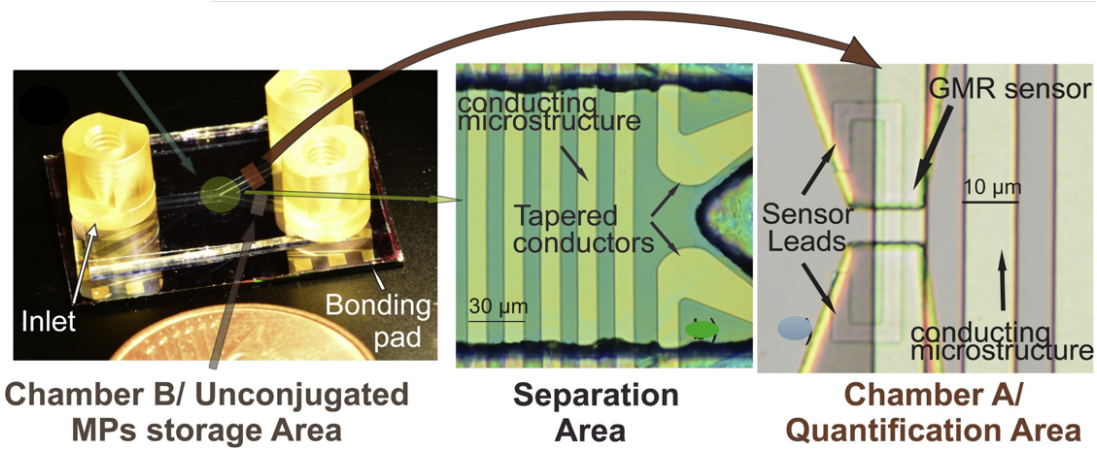

Figure 2-7 The integrated GMR sensor with Microfluidics Reprinted from ref. [195] Kokkinis et al. Sensors and Actuators B: Chemical, Vol. 241, 2017, pp. 438–445, with permission from Elsevier.

TMR is an interesting physical effect that has been attracting ample scientific attention in the past years. Simply put, TMR is an electrically measurable resistance change occurring when there is thin insulating film separating two magnetic materials. TMR is due to quantum mechanical electron tunnelling across the thin film and is similar to the GMR effect. Julliere discovered TMR for the first time in 1975 [196] by theoretically suggesting the large resistance change occurring when there is thin insulating film placed in the centre of the sandwich made from two ferromagnets. It was only in the 1990s, however, that the effect was utilized in magnetic read heads within Hard Disk (HDD) devices, where there was much

increased storage density. TMR is presently utilized in various applications, including magnetoresistive random access memory (MRAM), and magnetic sensors. Based on its characteristic behaviour, TMR has the benefits of low power consumption, short switching time, as well as non-volatility, and is even possible to pattern as a chip. Due to its interesting behaviour, TMR has been revolutionizing the area of study of spintronics and has tremendous potential across many technological applications, in particular for Biosensors-on-Chip (BoC) [197].

While both GMR and TMR sensors rely on spin-dependent electron transport, TMR offers greater signal contrast and is more suitable for integration with CMOS-compatible microfabrication. These attributes, simpler layer structure and lower noise, long with its mechanical robustness and miniaturization capability, made TMR the preferred choice for this project's sensing component. To the best of our knowledge, there is no previous report of the integration of a TMR sensor with a microfluidic system. Since this technique is intended for future work use in biological environments, the TMR sensor is used here in order to study how the sensor responds to variations in concentration of magnetic nanoparticles.

Chapter 3

3. Methodology

This chapter outlines the materials and methodologies utilized for the synthesis and fabrication of hydrogels and microfluidic devices with specific applications in sensing technology. The primary materials include GelMA, methacrylic anhydride (MA), and PEGDA, along with various chemical agents and nanoparticles, all sourced from reputable suppliers such as Sigma-Aldrich and CELLINK. PEGDA and GelMA were chosen for their complementary properties and compatibility with DLP-based photopolymerization. As mentioned before, GelMA, derived from natural gelatin, offers excellent biocompatibility and cell-adhesive features, making it a suitable candidate for biological integration. moreover, PEGDA, a synthetic and inert polymer, demonstrated superior printability and structural fidelity under DLP conditions. GelMA is synthesized through an intricate process involving the gradual incorporation of MA into a gelatine solution, followed by a series of dialysis and freeze-drying steps to prepare a suitable hydrogel for further applications. Complementary to GelMA and PEGDA hydrogel synthesis is executed to explore its potential in 3D printing applications. The methods section also details the photolithography processes employed in device fabrication, utilizing advanced techniques such as DLP printing and various characterization and testing setups designed to evaluate the functional capabilities of the developed materials. Each subsection provides precise, step-by-step descriptions necessary for replicating the procedures, ensuring clarity in the experimental design. Indeed, emphasis is placed on the synthesis of GelMA and PEGDA solutions, the preparation of magnetic nanoparticle dispersions, and the experimental setup for evaluating the sensing performance of the fabricated devices using a TMR sensor. By systematically detailing the methodologies, this chapter aims to provide a comprehensive understanding of the processes involved in developing the materials and structures essential for this research.

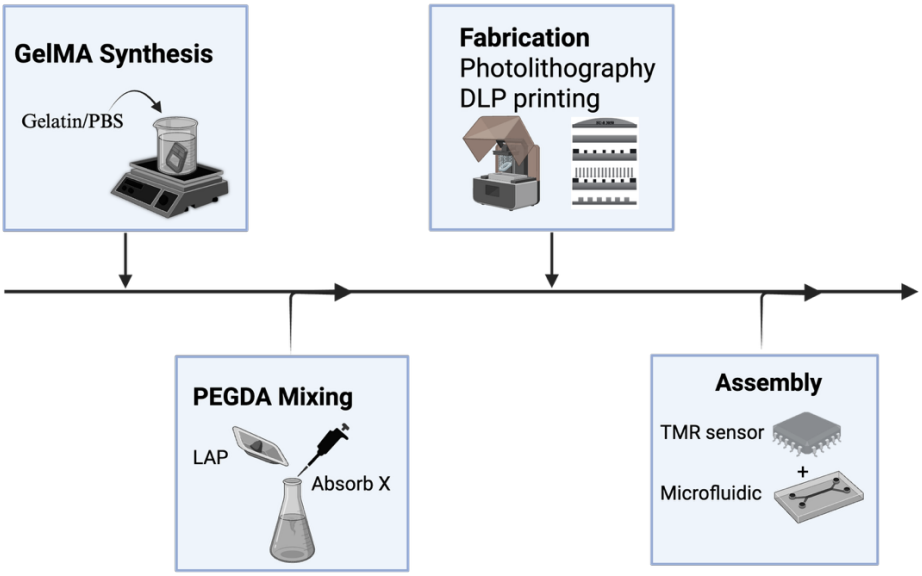

Figure 3-1 Schematic diagram to show process.

3.1. Materials and Methods

In this section, the materials and methodologies employed in the synthesis of GelMA and PEGDA hydrogels, were detailed essential for subsequent 3D printing applications. Our materials included high-quality gelatine (gel strength 300), MA, phosphate-buffered saline (PBS), and PEGDA (700 Mw), all sourced from Sigma-Aldrich, along with additional components such as the photoabsorber Xsorb from CELLINK and the photoinitiator lithium phenyl-2,4,6-trimethylbenzoylphosphinate (LAP). The methods outlined include the step-by-step synthesis of GelMA, followed by the preparation of GelMA and PEGDA hydrogels, ensuring optimal conditions for achieving desired properties. Synthesis protocols will be discussed in detail, including specific concentrations, stirring conditions, and the importance of light protection during the preparation phases.

3.1.1. GelMA synthesis

In this study, the synthesis of GelMA was performed following the methodology reported by [20]. A PBS tablet was dissolved in 500 mL of distilled water to prepare a PBS solution. 100 mL of the PBS was transferred into a container and placed on a hotplate set between 40°C and 60°C with a magnetic stirrer. Gelatine (10% w/v) was gradually added to the PBS solution while it was continuously stirred. The container was covered with aluminium foil to minimize evaporation and light exposure. The process of adding the gelatine and fully dissolving it in the solution was completed in approximately 1 hour. Methacrylic anhydride (MA) was slowly added drop by drop to the PBS and gelatine solution while it was continuously stirred. The entire container was securely covered with aluminium foil to block out light and prevent photodegradation. MA was added over approximately 45 minutes, and

the reaction was allowed to proceed for 3 hours to ensure completion of the synthesis. The solution was dialyzed for five days using cassettes containing cellulose membranes with a 12 kDa molecular weight cutoff (100). Dialysis was performed to remove unwanted by-products. The cassettes were placed in distilled water, and the water was replaced every hour to ensure effective dialysis. The dialyzed solution was pre-frozen at -20°C for 24 hours. Then, it was pre-frozen at -80°C for at least 24 hours. Finally, the solution was freeze-dried in a freeze-dryer for 48 hours.

3.1.2. Preparation of GelMA Solution for Printing

For printing synthesized GelMA using the LUMEN X bioprinter, a 10% w/v gelatine solution was prepared by dissolving 0.3 g of gelatine in 3 mL of PBS using a hot plate stirrer set to 50°C. After complete dissolution, the solution was transferred to a cooled stirrer, and 0.015 g of LAP was added as the photoinitiator to achieve a final concentration of 0.5% (w/v), as shown in Figure 3-2.

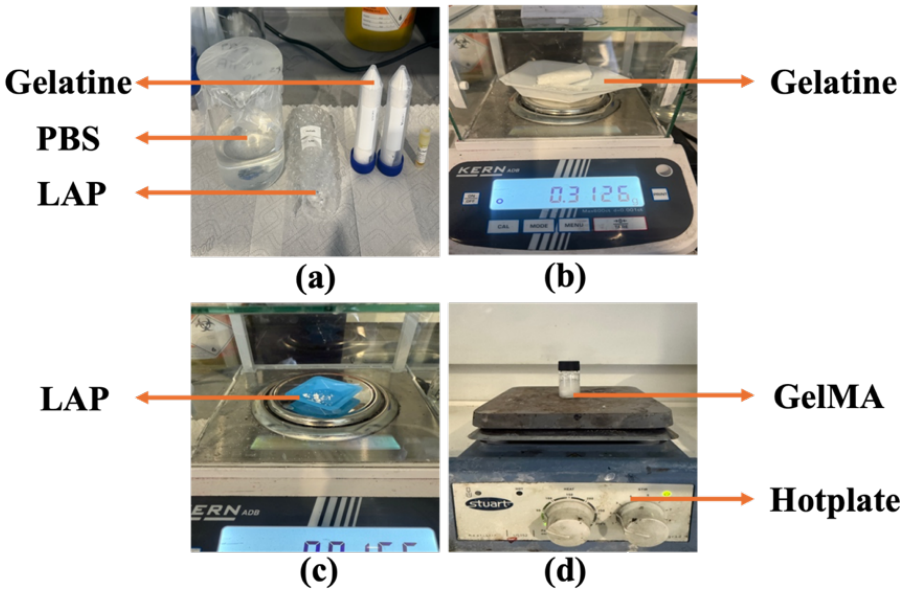

Figure 3-1 Preparation of a 10% (w/v) gelatine hydrogel.

To print this polymer, PEGDA (700 Mw) solutions with concentrations of 15%, 25%, and 35% (v/v) were prepared by combining PEGDA with PBS to a total volume of 3000 µL. The proportions for each concentration are presented in Table 3.1. All volumes were accurately measured using a 1000 µL pipette. Each mixture was placed on a magnetic stirrer for thorough mixing, with the container covered by aluminium foil to prevent light exposure. During stirring, 0.015 gr of LAP, a photoinitiator, and 60µL of AbsorbX (Cellink), a photoabsorber, were added to each solution. The mixtures were stirred continuously for two hours to ensure complete and uniform mixing, taken from [198].

Table 3-1 Proportions of PEGDA and PBS for different concentrations

Concentration	PEGDA(µl)	PBS(µl)
15%	450	2550
25%	750	2250
35%	1050	1950

Preliminary experiments using PEGDA at various concentrations (15%, 25%, 35%) revealed that a 25% solution yielded optimal resolution and mechanical strength. Together, these hydrogels provided a biodegradable foundation for device fabrication, aligning with the project's sustainability goals.

3.2. Fabrication

3.2.1. Photolithography Process

One of the conventional methods of microfluidic fabrication is based on the photolithography technique, which involves several key steps: (1) pre-cleaning, (2) photoresist (PR) coating, (3) pre-baking to harden the PR, (4) exposure, (5) development, (6) post-baking, followed by (7) etching, (8) PR stripping, and (9) post-cleaning (Figure 3-3). All fabrication steps were carried out in a cleanroom environment to minimize contamination and ensure process reliability. Firstly, the substrate was cleaned three times with acetone, isopropanol, and reverse-osmosis (RO) water, each step for five minutes. This step, known as the substrate cleaning phase, was performed to remove contaminants. Solvents such as acetone and isopropanol, along with deionized RO water were used to ensure a clean surface for subsequent processing steps. Next, the epoxy-based negative photoresist (SU-8) 3050 was spin-coated onto the substrate. This step, known as spin coating, involved applying SU-8 3050, a negative photoresist, to the substrate and spinning it at high speed to form a uniform, thick layer. SU-8 3050 was selected for its ability to create thick films (ranging from micrometres to millimetres), making it ideal for fabricating high-aspect-ratio structures. The substrate was baked for 45 minutes at 95°C (Figure 3-4 a). This step, known as the soft bake or pre-bake, was preformed to remove solvents from the SU-8 3050 photoresist, enhance adhesion, and prepare the film for exposure. A temperature of 95°C and a duration of 45-minutes were selected as standard conditions for SU-8 3050 to ensure effective solvent evaporation. Following this, the exposure step was carried out, during which the SU-8 3050 -coated substrate was exposed to UV light through a photomask using an MA6 mask aligner (Figure 3-4 b). For SU-8 3050 (a negative photoresist), the exposed areas were cross-linked and rendered insoluble, thereby defining the pattern. The post-exposure bake (PEB) was carried out, a critical step for SU-8 3050. The two-stage baking process was applied, starting at a lower temperature of 65°C to prevent thermal

shock, followed by heating at 95°C. This promoted cross-linking in the exposed regions and enhanced pattern fidelity and mechanical stability. The development step was performed to dissolve the unexposed SU-8 3050 (non-cross-linked regions) using ethyl lactate as the developer, thereby revealing the patterned structures. A second rinse with fresh ethyl lactate was performed to ensure complete removal of residual unexposed photoresist. Although, propylene glycol methyl ether acetate (PGMEA) is more commonly used, ethyl lactate was used as an alternative developer for SU-8 3050 [199]. The hard bake (or post-bake) was then conducted to further cross-link the SU-8 3050 structures, enhancing their thermal and mechanical stability (Figure 3-4, c). A high temperature of 180°C was applied, typical for SU-8 3050, to produce robust, permanent patterns suitable for subsequent processing (e.g., as Molds or structural components).

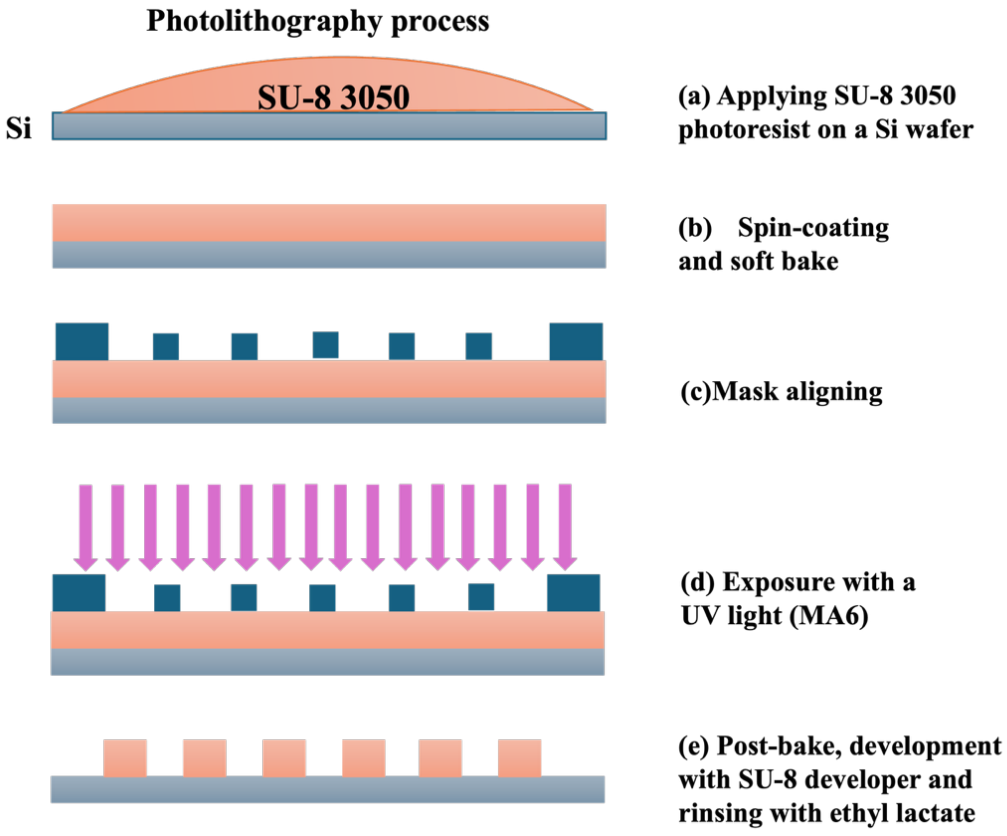

Figure 3-2 Photolithography process

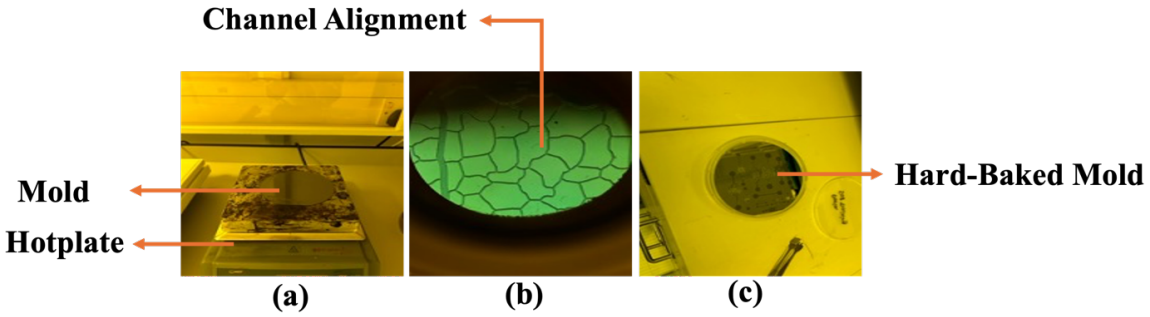

Figure 3-3 (a) Soft bake (b) Channel alignment, (c) Hard baked Mold.

PDMS Preparation

In this study PDMS was used to fabricate the microfluidic device. PDMS (purchased from Sigma-Aldrich) and SYLGARD^{TM} 184Silicone Elastomer curing agent were mixed at a 10:1 ratio in a plastic beaker and stirred vigorously for 10 minutes, resulting in the formation of numerous air bubbles. The mixture was then placed in a vacuum desiccator to remove the bubbles completely. Once degassed, the PDMS was slowly poured over the mold and curried in an oven 60°C for 2 hours. After curing, the microfluidic structure was cut using a blade, carefully removed from the mold, and bonded onto a thin glass substrate (Figure 3-5).

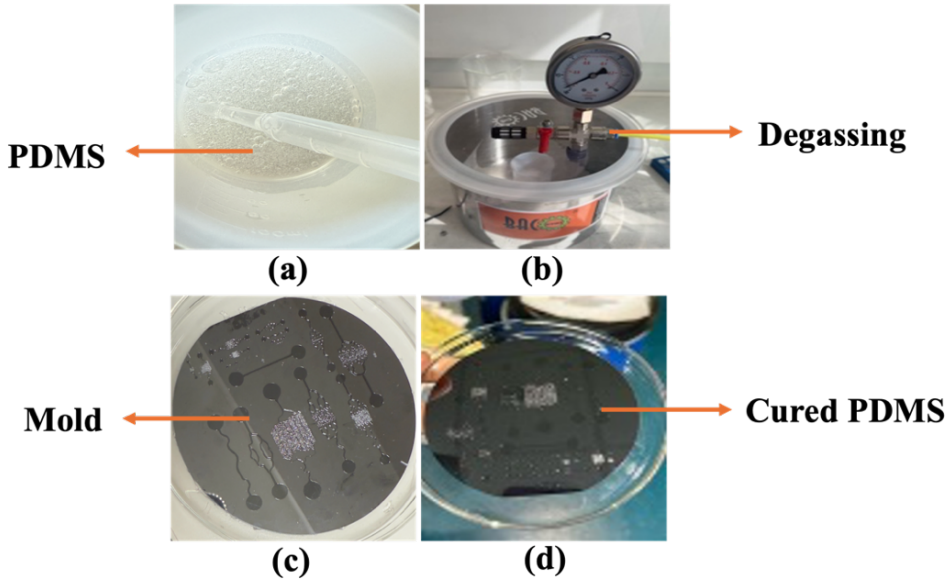

Figure 3-4 Preparation of PDMS microfluidic structure.

While the primary objective of this research was to develop biodegradable microfluidic platforms, PDMS was employed during early-phase fabrication to validate channel geometries and optimize the integration process with TMR sensors. PDMS's optical transparency, ease of molding, and established bonding techniques made it a practical choice for comparing with PEGDA-based structures. Its inclusion allowed for reliable prototyping before transitioning fully to biodegradable materials.

3.2.2. 3D digital light processing printing

3D structures were fabricated using DLP printing, a photopolymerization-based technique that enables high-resolution printing of photocurable materials. A Cellink Lumen X DLP printer (Cellink, Sweden), shown in (Figure 3-6, a), was used for this purpose. The printer utilizes a digital light projector to selectively cure liquid resin layer by layer, offering precise control over the geometry and resolution of the printed structures. The PEGDA solutions with concentrations of 15%, 25%, and 35% (v/v), prepared as mentioned in Section 3.1.3, were used as the printing resins. Each solution contained LAP as a photoinitiator and AbsorbX (Cellink) as a photoabsorber to control light penetration and ensure accurate curing. The 3D models were designed using Autodesk Fusion 360 software and exported as .STL files. To enhance the printing parameters for the production of high-resolution and structurally robust structures, several combinations of layer thickness and exposure duration were methodically assessed. Exposure lengths of 2, 3, and 5 seconds for each layer were evaluated. An exposure duration of 2 seconds led to inadequate curing and compromised structural integrity, whereas 3 and 5 seconds produced appropriate outcomes, with 5 seconds enhancing feature definition and uniformity. Similarly, layer thicknesses of 20 µm (Figure 3-6 b), 50 µm (Figure 3-6 c), and 100 µm were evaluated. The thinner layers (20 and 50 µm) resulted in extended printing durations and sporadic layer delamination, with no improvement in resolution. A layer thickness of 100 µm yielded well-defined and mechanically robust constructions, thus being designated as the best setting. Consequent to these results, a layer thickness of 100 µm and an exposure duration of 5 seconds were used in all ensuing prints to guarantee thorough curing, structural integrity, and printing efficacy. Printing occurred at room temperature under standard laboratory circumstances, with the printer's orange protective cover (Figure 3-6) safeguarding the resin from ambient light disruption. Subsequent to creation, the printed structures were meticulously removed off the build platform and washed with isopropyl alcohol (IPA) to eradicate any uncured resin. A post-curing procedure was then performed using a 365 nm UV light for 5 minutes to augment mechanical stability and ensure thorough crosslinking.

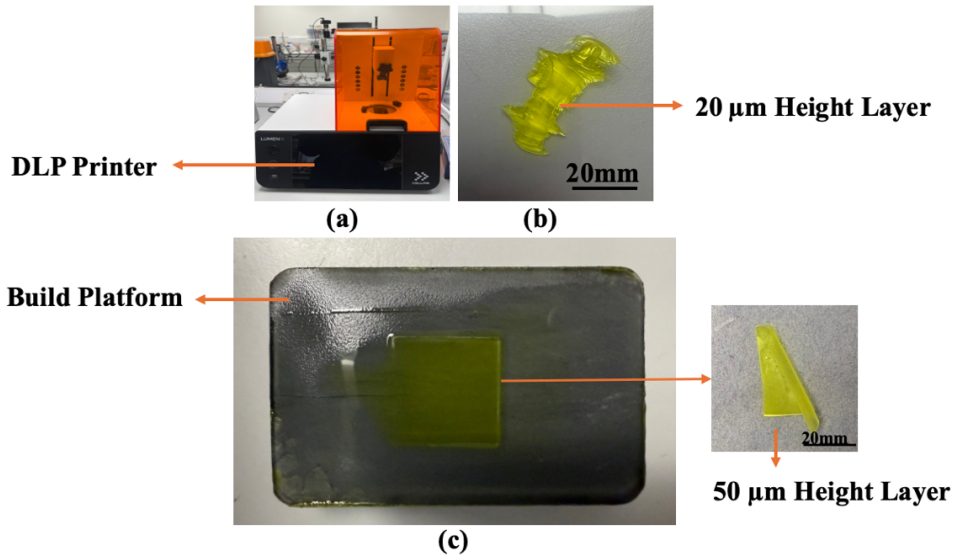

Figure 3-5 (a) Cellink Lumen X DLP printer, (b) Structure printed with 20 µm layer height, (c) Structure printed with 50 µm layer height.

Both photolithography and digital light processing (DLP) 3D printing were employed in this study to enable a comparative analysis of their fabrication performance for microfluidic devices. Photolithography, a conventional and widely accepted technique, was used to create PDMS molds with high fidelity, especially for initial prototyping and alignment trials. DLP printing, on the other hand, offered the advantage of rapid, maskless, and high-resolution fabrication using photocurable biodegradable hydrogels such as PEGDA. By applying both methods, this study aimed to evaluate in resolution, scalability, material compatibility, and fabrication speed. The comparison revealed that DLP printing with PEGDA provided superior geometric precision and printability, making it more suitable for eco-friendly, high-resolution biodegradable biosensing platforms.

3.3. Sensing Application

The fabricated microfluidic platform was evaluated for sensing applications using an electromagnetic setup comprising a TMR sensor and a semiconductor analyser (Keithley 2450). To assess the performance of microfluidic exposed to the TMR sensor, various concentrations of MNPs were prepared and introduced into the microfluidic channel. MNPs: Fe_3O_4 solution was prepared by dissolving iron (II, III) oxide nanopowder with a particle size of 50-100 nm and a 97% trace metals basis in deionized (DI) water at various concentrations between 5000 to 40000 µg/mL. The solutions were ultrasonicated for 30 minutes to ensure complete dispersion.

The setup was shown in Figure 3-7 (A, B). In this setup, to reduce the influence of environmental conditions on motion artifacts, magnetically shielded chamber (Twinleaf-MS2) was used to create a controlled experimental setup [200]. This chamber features four

layers of high-permeability metal shielding, which help block out ambient magnetic noise from electronic devices and other lab equipment that could interfere with the magnetic measurements. Inside, it has coils with a diameter of 180 mm and length of 360 mm, allowing to precisely adjust the magnetic field within the chamber. The current needed in the coils to produce the desired magnetic field, the so-called conversion factor, is 56.5 nT/mA for uniform fields and 1.82 nT/cm/mA for magnetic gradients. To prevent any mechanical vibrations from affecting the measurements, the chamber was placed on a separate, damped optical table.

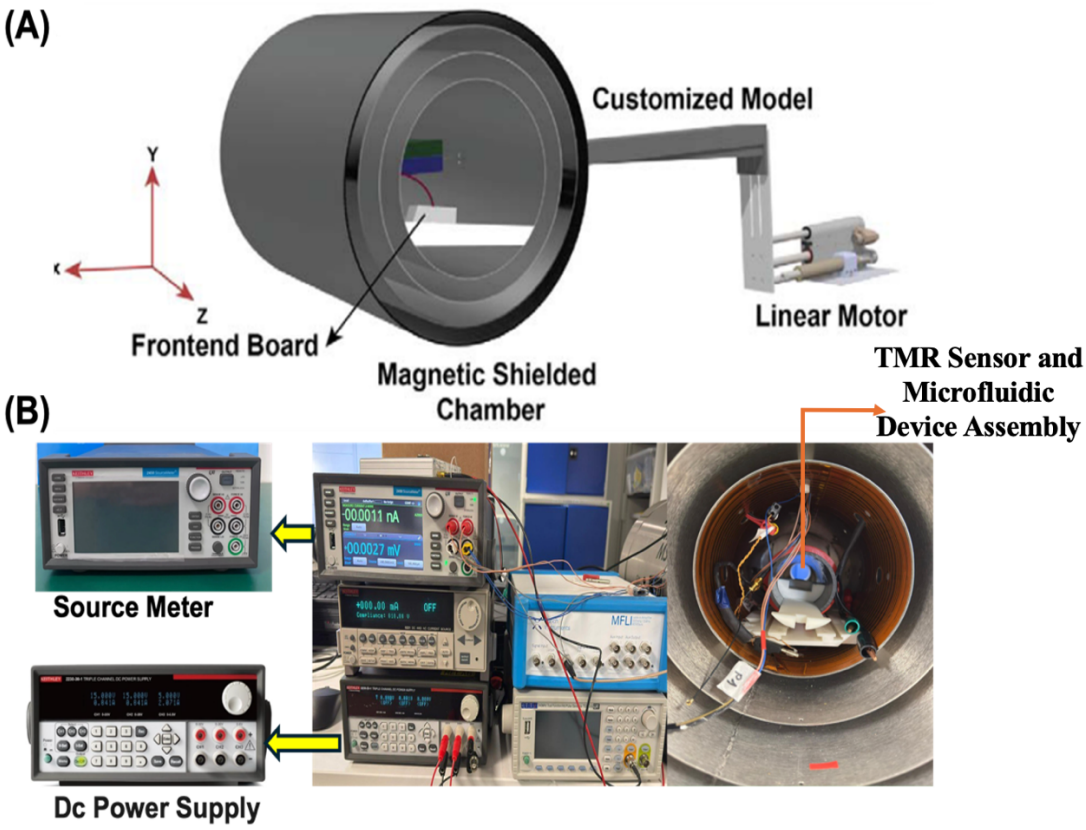

Figure 3-6 (A)schematic diagram of Twinleaf-MS2 magnetically shielded chamber. Adopted from ref.[200], Ghahremani Arekhloo et al 2024, under the terms of the Creative Commons Attribution License [CC BY 4.0]. (B) The used original measurement setup.

The sensing performance was evaluated under a constant voltage mode (3 V), where the current response was monitored as a function of MNP concentration. Initially, the baseline current was established by introducing deionized (DI) water into the channel under a constant magnetic field and voltage, and the corresponding current was recorded. Subsequently, MNP suspensions at concentrations ranging from 5,000 to 40,000 µg/mL were thoroughly vortexed and gently introduced into the channel. After allowing a 2-minute reaction time, the current was recorded under the same magnetic field 6.5pT and voltage conditions. Following each measurement, the channel was flushed twice with DI water using a syringe until the current returned to the baseline level, ensuring removal of residual MNPs

before introducing the next concentration. Upon testing all concentrations, a calibration curve was generated to evaluate the sensing performance of the platform. Additionally, the dynamic behaviour of the system during sample injection was analysed to assess real-time response characteristics.

TMR sensors were used for their high sensitivity, low power consumption, and robustness in detecting magnetic fields compared to alternative magnetic sensors such as GMR. The high signal-to-noise ratio and excellent linearity in response to magnetic nanoparticle concentrations made TMR particularly suitable for precise biosensing in microfluidic platforms. These attributes aligned with the project's goal of achieving high-performance, low-cost diagnostics.

Chapter 4

4. Results and Discussion

4.1. PEGDA printing

First, we evaluated the potential of printing microfluidic devices using the commercial PEGDA X resin with the Cellink Lumen X DLP printer. The results were promising for fabricating biodegradable microfluidic platforms. Microfluidic channels with precise dimensions, width of 0.5 mm, depth of 1 mm, length of 10 mm, and inlet/outlet diameters of 1 mm, were successfully produced, demonstrating the efficacy of PEGDA X as a reliable material for high-resolution prototyping. The printing process employed optimized parameters, including a layer thickness of 100 µm, an exposure time of 10 seconds per layer, and a light intensity of 70, as established in prior methodology (Section 3.2.2). These findings, illustrated in (Figure 4-1), underscore the potential of PEGDA X for reproducible and scalable production of microfluidic devices, offering consistent material properties and well-defined channel geometries essential for applications in biosensing and tissue engineering.

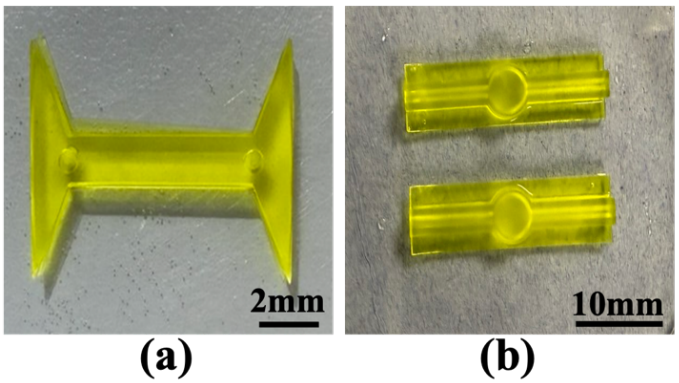

Figure 4-1 PEGDA X: (a) Channel size: Width: 0.5mm, Depth: 1mm, Length:10mm, Inlet = 1mm, Outlet = 1mm (b) Channel size: Width:1mm, Depth:1mm, Length:30mm, Inlet = 1mm, Outlet = 1mm

Then, based on the experiments with different percentages of PEGDA solution, only the PEGDA 25% was suitable for fabricating microfluidic devices, displaying output and behaviour comparable to the commercial PEGDA X, as shown in Figure 4-2. For printing PEGDA 25% using the LUMEN X bioprinter, PEGDA (700 Mw) in PBS was prepared. Then, 0.5% w/v LAP was added to the PEGDA solution as the photoinitiator. The printing procedure was conducted with a light intensity of 70% and a light exposure time of 3 seconds per layer. The LUMEN X provide the light with the wavelength of 405, so LAP photoinitiator was employed. With this optimized PEGDA percentage, printing biodegradable microfluidic devices with a channel size of 0.5 mm is now achievable.

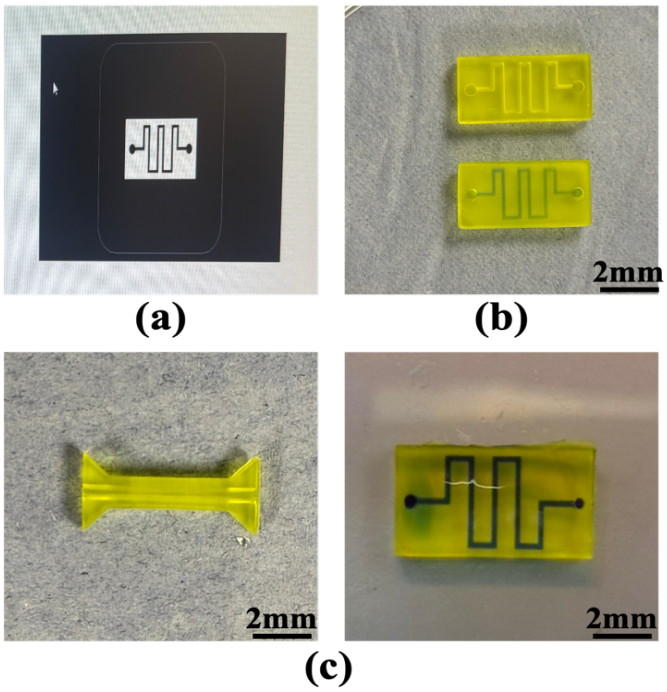

Figure 4-2 PEGDA 25% hydrogel printed with Lumen X bioprinter: (a) Designed channel, (b and c) different patterns of microfluidics

Among these, the 25% PEGDA solution demonstrated the best performance in terms of resolution and layer fidelity. This is likely due to its balanced viscosity and photoreactivity, which allowed for accurate polymerization during DLP printing. In contrast, 15% PEGDA was too fluid, leading to spreading and blurred edges, while 35% PEGDA was too viscous, resulting in incomplete curing. These findings are consistent with other studies [201], that reported optimal printability in the 20–30% PEGDA range. This outcome supports the project objective of selecting a biodegradable hydrogel with good resolution for high-quality microchannel fabrication.

4.2. GelMA printing

Firstly, to test the gelation of synthesized GelMA, 10\% w/v solution of GelMA with 0.5\% w/v Irgacure 2959 was prepared, and the curing was performed in a Crosslinker XL-1500 365 nm. The UV exposure was 30 seconds. The reason for using Irgacure 2959 was that the curing device's light wavelength was 365 nm. The successfully cured (crosslinked) GelMA and the testing steps are presented in Figure 4-3 (a, b).

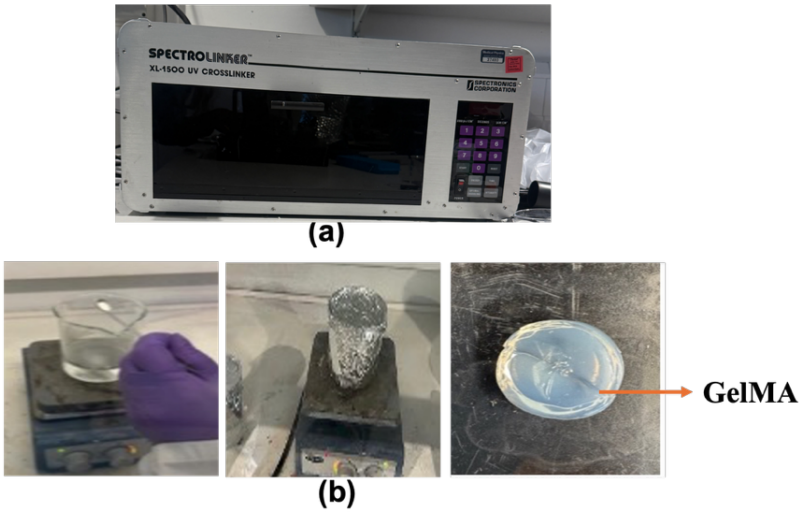

Figure 4-3 (a) Crosslinker XL-1500 (b) Crosslinked GelMA with Irgacure 2959 as the photoinitiator and in a UV crosslinker box.

For printing synthesized GelMA using the LUMEN X bioprinter, 10\% w/v GelMA in PBS was prepared. Printing of Cellinks GelMA was performed by LUMEN X not only for training goals and to learn to work with the printer but also to get acquainted with the printing properties and parameters related to the mentioned materials.

Although full printing of the synthesized GelMA was not completed, the material was successfully crosslinked using a UV source, confirming its potential compatibility with photopolymerization techniques. These initial tests contribute to understanding the material's limitations and guide future optimization efforts for using GelMA in biodegradable microfluidic fabrication.

4.3. Photolithography

Fig. 4.4 (a) displays a clear microfluidic chip in a Petri dish, illustrating their dimensional accuracy and cleanliness after the fabrication process. The second image features a single chip being held, emphasizing its robust design and clarity, which are crucial for visualizing the internal channel patterns. Figure 4-4 (b) provides a close-up view of one of the microchannels, revealing sharp edges and precise features that demonstrate the effectiveness of the photolithography method used. Overall, these results indicate that the fabrication process was successful, yielding high-quality microfluidic devices suitable for various applications in research and diagnostics.

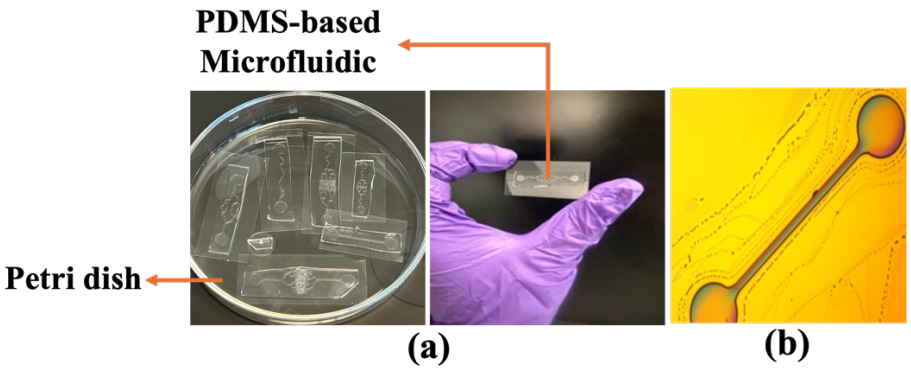

Figure 4-4 (a) Multiple microfluidics. (b) A magnified view of a microchannel

This method served as a benchmark to compare with 3D printed hydrogels, highlighting differences in resolution, material behavior, and fabrication speed. While not biodegradable, PDMS devices produced through photolithography offer a reference for structural integrity and channel definition.

4.4. TMR Sensor Performance

The results show that as the concentration of MNPs increases, the current response initially rises in a predictable, linear manner, indicated by the high R^2 value of 0.9771, demonstrating good calibration for quantification (Figure 4-5). At higher concentrations, the curve begins to plateau, suggesting a saturation point where additional MNPs no longer significantly influence the current. The analysis of the system's behaviour during sample injection also provided insights into its responsiveness and stability in real-time detection scenarios. Overall, these results highlight the sensor's capability to accurately detect varying MNP concentrations within the tested range, with reliable and reproducible performance.

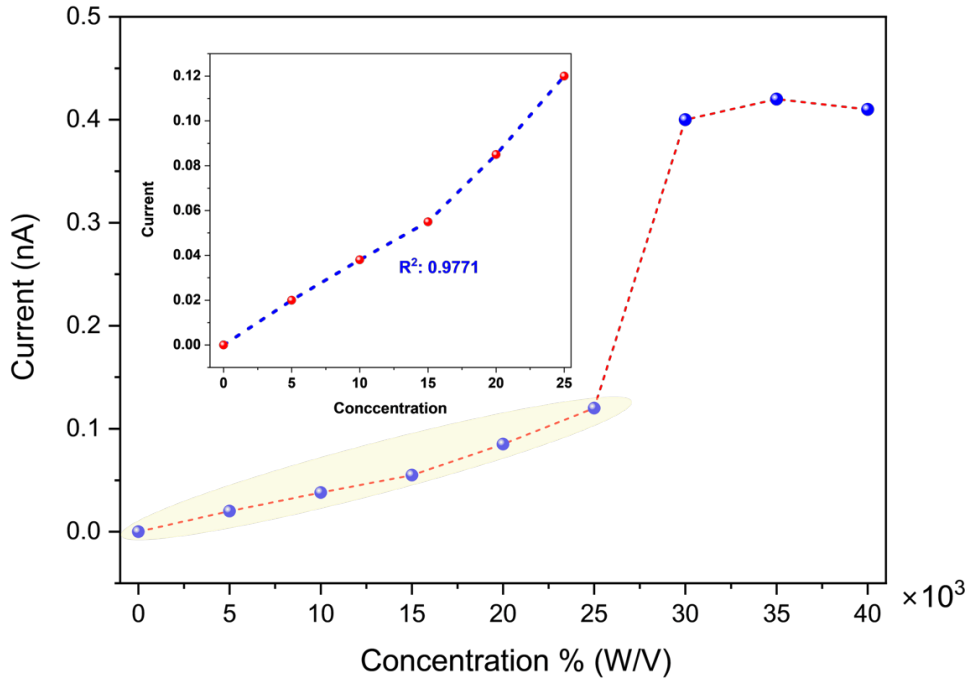

Figure 4-5 TMR sensor response to the MNP different concentration with calibration curve showing the linear relationship between MNP concentration

Figure 4-6 demonstrates the current response of a sensing system over time while different samples are introduced. At the beginning, the baseline current is established with no sample present. When the "Sample 1" is introduced (green highlighted region), there is an immediate jump in current, indicating the sensor's response to the sample. After the sample is removed and the sensor is flushed (green region), the current drops back to the baseline. This process is repeated for successive samples, Sample 2 (blue region) and Sample 3 (purple region), each resulting in a stepwise increase in current upon introduction, followed by a return to baseline after flushing. The clear step changes confirm that the sensor is responsive to the presence of each sample and returns reliably to the baseline between exposures, demonstrating good selectivity and repeatability in performance.

Sensitivity is a signeficant parameter in evaluating a sensor's performance and is typically determined from the slope of a linear calibration curve. When the sensor output (such as voltage, resistance, or current) is plotted against the applied stimulus (such as analyte concentration, pressure, or magnetic field), a linear relationship often appears. The slope of this linear curve represents the sensor's sensitivity, indicating how much the output changes per unit change in the input. A steeper slope corresponds to higher sensitivity, meaning the sensor can more effectively detect small variations in the stimulus. According to this measurement, sensitivity of designed platform was calculated 0.0047 nA/µg(mL)$^{-1}$.

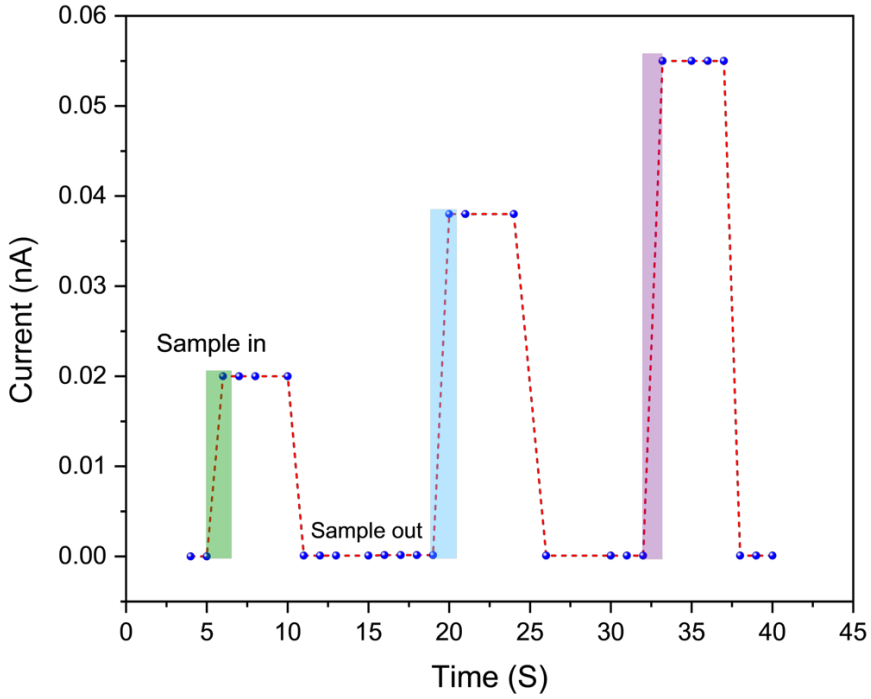

Figure 4-6 TMR sensor response to the MNP by implying the current response of the sensing system during sequential introduction and flushing of different samples.

The TMR sensor exhibited a clear linear response to increasing concentrations of MNPs in the range of 0 to 40 × 10^3, with a correlation coefficient of $R^2 = 0.9771$. This strong linearity indicates high sensitivity and stability in signal detection. The performance can be attributed to the inherent properties of TMR sensors, including low noise, sharp resistance transitions, and minimal interference. Compared to other magnetic sensing technologies such as GMR, TMR sensors offer enhanced resolution and signal clarity, especially at low field strengths. These results confirm the suitability of TMR technology for microfluidic biosensing applications and support the core objective of this project to develop an integrated, high sensitivity biosensing platform for real-time detection.

Chapter 5

5. Conclusion and Future Trends

In this study, we focused on developing hydrogels and microfluidic devices by using two innovative materials: GelMA and PEGDA. These hydrogels were chosen because of their notable biocompatibility, tunable properties, and suitability for creating detailed microstructures. Through careful synthesis and optimization, we were able to prepare GelMA and PEGDA solutions with the right viscosity and composition for use in advanced fabrication methods. In particular, 25% PEGDA was identified as the optimal concentration for DLP printing, producing microchannels with 500 µm width and 1 mm depth.

A major achievement of this work was demonstrating that both GelMA and PEGDA can be effectively used in 3D printing technologies, particularly digital light projection printing. By optimizing the printing parameters, such as layer thickness, exposure time, and photoinitiator concentration, we successfully produced microfluidic devices with well-defined, smooth channels and reproducible geometries. These channels are essential for precisely controlling the flow of liquids, which is a key requirement in many sensing and diagnostic applications.

The TMR sensor achieved a linear detection response in the 0–40 × 10^3 MNP concentration range, with $R^2 = 0.9771$, demonstrating strong correlation and sensitivity.
The performance of our microfluidic platforms was tested with a TMR sensor, which accurately detected various concentrations of MNPs. The sensor showed high sensitivity and reliable results across different trials, suggesting that our devices could be valuable for real-time applications in fields like healthcare and environmental monitoring. The sensing experiments demonstrated the TMR sensor's capability to detect magnetic signals appeared by the flowing of magnetic nanoparticle through the microfluidic channel from a under controlled conditions.

The setup ensured proper alignment of the sensor's sensitivity direction and accounted for noise interference by analysing data in the 102–103 Hz range. Further optimization may involve the thinning the measuring side of microfluidic platform. The reliability and repeatability of these responses across multiple trials highlight the robustness of both the fabricated devices and the sensing setup. These findings suggest that our approach could be used not only for experimental research but also for real-world applications where rapid and accurate sensing is critical. Such applications include medical diagnostics, where detecting specific biomarkers is essential, as well as environmental monitoring, where quick identification of contaminants or nanoparticles can help ensure public safety.

Looking to the future, we expect several exciting trends in microfluidics and sensing technology. New materials may emerge that offer better mechanical properties and specific functions, enhancing the capabilities of microfluidic devices. Additionally, integrating smart technologies such as artificial intelligence could streamline data analysis, making sensing systems even more intuitive and effective. We also foresee advancements in multi-material printing techniques, which could allow more complex microfluidic systems with additional functionalities. As sustainability becomes increasingly important, the use of biodegradable materials like PEGDA reflects a positive shift towards environmentally friendly practices in technology.

References

[1] B. Senf, W.-H. Yeo, and J.-H. Kim, "Recent advances in portable biosensors for biomarker detection in body fluids," *Biosensors,* vol. 10, no. 9, p. 127, 2020.

[2] A. I. Barbosa, R. Rebelo, R. L. Reis, M. Bhattacharya, and V. M. Correlo, "Current nanotechnology advances in diagnostic biosensors," *Medical Devices & Sensors,* vol. 4, no. 1, p. e10156, 2021.

[3] A. Pulumati, A. Pulumati, B. S. Dwarakanath, A. Verma, and R. V. Papineni, "Technological advancements in cancer diagnostics: Improvements and limitations," *Cancer Reports,* vol. 6, no. 2, p. e1764, 2023.

[4] M. A. Mujawar, H. Gohel, S. K. Bhardwaj, S. Srinivasan, N. Hickman, and A. Kaushik, "Nano-enabled biosensing systems for intelligent healthcare: towards COVID-19 management," *Materials Today Chemistry,* vol. 17, p. 100306, 2020.

[5] J. Wu, H. Liu, W. Chen, B. Ma, and H. Ju, "Device integration of electrochemical biosensors," *Nature Reviews Bioengineering,* vol. 1, no. 5, pp. 346-360, 2023.

[6] A. Kowalczyk, "Trends and perspectives in DNA biosensors as diagnostic devices," *Current Opinion in Electrochemistry,* vol. 23, pp. 36-41, 2020.

[7] Z. Liu *et al.*, "Microfluidic biosensors for biomarker detection in body fluids: a key approach for early cancer diagnosis," *Biomarker Research,* vol. 12, no. 1, pp. 1-29, 2024.

[8] C. M. Pandey *et al.*, "Microfluidics based point-of-care diagnostics," *Biotechnology journal,* vol. 13, no. 1, p. 1700047, 2018.

[9] D. Barata, C. van Blitterswijk, and P. Habibovic, "High-throughput screening approaches and combinatorial development of biomaterials using microfluidics," *Acta biomaterialia,* vol. 34, pp. 1-20, 2016.

[10] L. Mathur, M. Ballinger, R. Utharala, and C. A. Merten, "Microfluidics as an enabling technology for personalized cancer therapy," *Small,* vol. 16, no. 9, p. 1904321, 2020.

[11] T. Murthy and D. Yeo, "Life sciences discovery and technology highlights," *SLAS technology,* vol. 27, no. 1, pp. 94-96, 2022.

[12] S. Choi, M. Goryll, L. Y. M. Sin, P. K. Wong, and J. Chae, "Microfluidic-based biosensors toward point-of-care detection of nucleic acids and proteins," *Microfluidics and Nanofluidics,* vol. 10, pp. 231-247, 2011.

[13] L. Y. Yeo, H. C. Chang, P. P. Chan, and J. R. Friend, "Microfluidic devices for bioapplications," *small,* vol. 7, no. 1, pp. 12-48, 2011.

[14] M. I. Hajam and M. M. Khan, "Microfluidics: a concise review of the history, principles, design, applications, and future outlook," *Biomaterials Science,* vol. 12, no. 2, pp. 218-251, 2024.

[15] S. Amir, A. Arathi, S. Reshma, and P. Mohanan, "Microfluidic devices for the detection of disease-specific proteins and other macromolecules, disease modelling and drug development: A review," *International Journal of Biological Macromolecules,* vol. 235, p. 123784, 2023.

[16] Q. Zhong, H. Ding, B. Gao, Z. He, and Z. Gu, "Advances of microfluidics in biomedical engineering," *Advanced materials technologies,* vol. 4, no. 6, p. 1800663, 2019.

[17] J. Sengupta, "Natural biodegradable polymers transforming lab on a chip technology: A mini review," *Green Analytical Chemistry,* p. 100119, 2024.

[18] S. B. Campbell, Q. Wu, J. Yazbeck, C. Liu, S. Okhovatian, and M. Radisic, "Beyond polydimethylsiloxane: alternative materials for fabrication of organ-on-a-chip devices and microphysiological systems," *ACS biomaterials science & engineering,* vol. 7, no. 7, pp. 2880-2899, 2020.
[19] D. T. Tran, A. S. Yadav, N. K. Nguyen, P. Singha, C. H. Ooi, and N. T. Nguyen, "Biodegradable polymers for micro elastofluidics," *Small,* vol. 20, no. 39, p. 2303435, 2024.
[20] P. Shukla, M. Mitruka, and F. Pati, "The effect of the synthetic route on the biophysiochemical properties of methacrylated gelatin (GelMA) based hydrogel for development of GelMA-based bioinks for 3D bioprinting applications," *Materialia,* vol. 25, p. 101542, 2022.
[21] K. Han, Y. Cheng, Q. Han, and J. Chen, "Extraction of type I collagen and development of collagen methacryloyl (ColMA)/PEGDA ink for digital light processing printing," *International Journal of Biological Macromolecules,* vol. 282, p. 137253, 2024.
[22] U. A. Gurkan *et al.*, "Next generation microfluidics: fulfilling the promise of lab-on-a-chip technologies," *Lab on a Chip,* vol. 24, no. 7, pp. 1867-1874, 2024.
[23] N. Sinha, N. Subedi, and J. Tel, "Integrating immunology and microfluidics for single immune cell analysis," *Frontiers in immunology,* vol. 9, p. 2373, 2018.
[24] L. F. Horowitz, A. D. Rodriguez, T. Ray, and A. Folch, "Microfluidics for interrogating live intact tissues," *Microsystems & Nanoengineering,* vol. 6, no. 1, p. 69, 2020.
[25] A. Kulasinghe, H. Wu, C. Punyadeera, and M. E. Warkiani, "The use of microfluidic technology for cancer applications and liquid biopsy," *Micromachines,* vol. 9, no. 8, p. 397, 2018.
[26] J. W. Lathrop, "The diamond ordnance fuze laboratory's photolithographic approach to microcircuits," *IEEE Annals of the History of Computing,* vol. 35, no. 1, pp. 48-55, 2011.
[27] A. Manz, N. Graber, and H. M. Widmer, "Miniaturized total chemical analysis systems: a novel concept for chemical sensing," *Sensors and actuators B: Chemical,* vol. 1, no. 1-6, pp. 244-248, 1990.
[28] S. Tomar, S. Sirame, and S. P. Choudhary, "3D Printing: Printing Future Food," *https://agritechmagazine. com,* vol. 8, p. 184, 2024.
[29] S. C. Terry, J. H. Jerman, and J. B. Angell, "A gas chromatographic air analyzer fabricated on a silicon wafer," *IEEE transactions on electron devices,* vol. 26, no. 12, pp. 1880-1886, 1979.
[30] A. W. Martinez, S. T. Phillips, M. J. Butte, and G. M. Whitesides, "Patterned paper as a platform for inexpensive, low-volume, portable bioassays," *Angewandte Chemie,* vol. 119, no. 8, pp. 1340-1342, 2007.
[31] S. Laleh, B. Ibarlucea, M. Stadtmüller, G. Cuniberti, and M. Medina-Sánchez, "Portable microfluidic impedance biosensor for SARS-CoV-2 detection," *Biosensors and Bioelectronics,* vol. 236, p. 115362, 2023.
[32] H.-B. Wu *et al.*, "Highly-specific aptamer targeting SARS-CoV-2 S1 protein screened on an automatic integrated microfluidic system for COVID-19 diagnosis," *Analytica Chimica Acta,* vol. 1274, p. 341531, 2023.
[33] S. A. Muhsin *et al.*, "A microfluidic biosensor architecture for the rapid detection of COVID-19," *Analytica Chimica Acta,* vol. 1275, p. 341378, 2023.
[34] C. L. Hisey, K. D. P. Dorayappan, D. E. Cohn, K. Selvendiran, and D. J. Hansford, "Microfluidic affinity separation chip for selective capture and

release of label-free ovarian cancer exosomes," *Lab on a Chip,* vol. 18, no. 20, pp. 3144-3153, 2018.
[35] T. Komatsu, M. Tokeshi, and S.-K. Fan, "Determination of blood lithium-ion concentration using digital microfluidic whole-blood separation and preloaded paper sensors," *Biosensors and Bioelectronics,* vol. 195, p. 113631, 2022.
[36] S. Hettiarachchi *et al.*, "Design and development of a microfluidic droplet generator with vision sensing for lab-on-a-chip devices," *Sensors and Actuators A: Physical,* vol. 332, p. 113047, 2021.
[37] L. Pan, *Complex fluids in microchannel flows at low Reynolds number: Elastic instabilities and rheology*. University of Pennsylvania, 2013.
[38] B. Zhao, C. W. MacMinn, and R. Juanes, "Wettability control on multiphase flow in patterned microfluidics," *Proceedings of the National Academy of Sciences,* vol. 113, no. 37, pp. 10251-10256, 2016.
[39] L. Chen, C. Zhang, V. Yadav, A. Wong, S. Senapati, and H.-C. Chang, "A home-made pipette droplet microfluidics rapid prototyping and training kit for digital PCR, microorganism/cell encapsulation and controlled microgel synthesis," *Sci Rep,* vol. 13, no. 1, p. 184, 2023.
[40] H. E. Estarki, Z. S. Tareie, and H. Latifi, "Pressure drop measurement in microfluidics channel by the Fabry-Perot diaphragm-based flow sensor," *Flow Measurement and Instrumentation,* vol. 91, p. 102355, 2023.
[41] K. Iwai *et al.*, "Scalable and automated CRISPR-based strain engineering using droplet microfluidics," *Microsystems & nanoengineering,* vol. 8, no. 1, p. 31, 2022.
[42] X. Fan, X. Zhang, and J. Ping, "Graphene-Enabled High-Performance Electrokinetic Focusing and Sensing," *ACS nano,* vol. 16, no. 7, pp. 10852-10858, 2022.
[43] S. S. Sahu, C. Stiller, S. Cavallaro, A. E. Karlström, J. Linnros, and A. Dev, "Influence of molecular size and zeta potential in electrokinetic biosensing," *Biosensors and Bioelectronics,* vol. 152, p. 112005, 2020.
[44] D. S. Rocha, R. P. de Campos, H. A. Silva-Neto, G. F. Duarte-Junior, F. Bedioui, and W. K. Coltro, "Digital microfluidic platform assembled into a home-made studio for sample preparation and colorimetric sensing of S-nitrosocysteine," *Analytica Chimica Acta,* vol. 1254, p. 341077, 2023.
[45] A. Tiribocchi, M. Durve, M. Lauricella, A. Montessori, D. Marenduzzo, and S. Succi, "The crucial role of adhesion in the transmigration of active droplets through interstitial orifices," *Nature Communications,* vol. 14, no. 1, p. 1096, 2023.
[46] A. Pomeransky and I. Khriplovich, "Equations of motion of spinning relativistic particle in external fields," *Surveys in High Energy Physics,* vol. 14, no. 1-3, pp. 145-173, 1999.
[47] R. P. Chhabra and V. Shankar, *Coulson and Richardson's Chemical Engineering: Volume 1A: Fluid Flow: Fundamentals and Applications*. Butterworth-Heinemann, 2017.
[48] W. S. Low, N. A. Kadri, and W. A. B. B. Wan Abas, "Computational Fluid Dynamics Modelling of Microfluidic Channel for Dielectrophoretic BioMEMS Application," *The Scientific World Journal,* vol. 2014, pp. 1-11, 2014, doi: 10.1155/2014/961301.
[49] F. Mi *et al.*, "Recent advancements in microfluidic chip biosensor detection of foodborne pathogenic bacteria: a review," *Analytical and Bioanalytical Chemistry,* vol. 414, no. 9, pp. 2883-2902, 2022.
[50] K. Raj M and S. Chakraborty, "PDMS microfluidics: A mini review," *Journal of Applied Polymer Science,* vol. 137, no. 27, p. 48958, 2020.

[51] B. K. Gale *et al.*, "A review of current methods in microfluidic device fabrication and future commercialization prospects," *Inventions,* vol. 3, no. 3, p. 60, 2018.
[52] J. Hwang, Y. H. Cho, M. S. Park, and B. H. Kim, "Microchannel fabrication on glass materials for microfluidic devices," *International Journal of Precision Engineering and Manufacturing,* vol. 20, pp. 479-495, 2019.
[53] P. N. Nge, C. I. Rogers, and A. T. Woolley, "Advances in microfluidic materials, functions, integration, and applications," *Chemical reviews,* vol. 113, no. 4, pp. 2550-2583, 2013.
[54] F. Kotz *et al.*, "Liquid PMMA: A high resolution polymethylmethacrylate negative photoresist as enabling material for direct printing of microfluidic chips," *Advanced Engineering Materials,* vol. 20, no. 2, p. 1700699, 2018.
[55] I. Bilican and M. T. Guler, "Assessment of PMMA and polystyrene based microfluidic chips fabricated using CO2 laser machining," *Applied Surface Science,* vol. 534, p. 147642, 2020.
[56] Y. Yajima, M. Yamada, E. Yamada, M. Iwase, and M. Seki, "Facile fabrication processes for hydrogel-based microfluidic devices made of natural biopolymers," *Biomicrofluidics,* vol. 8, no. 2, 2014.
[57] N. Gorenkova *et al.*, "The innate immune response of self-assembling silk fibroin hydrogels," *Biomaterials Science,* vol. 9, no. 21, pp. 7194-7204, 2021.
[58] M. Zhou *et al.*, "Self-Propelled and Targeted Drug Delivery of Poly(aspartic acid)/Iron–Zinc Microrocket in the Stomach," *ACS Nano,* vol. 13, no. 2, pp. 1324-1332, 2019/02/26 2019, doi: 10.1021/acsnano.8b06773.
[59] G. E. Luckachan and C. Pillai, "Biodegradable polymers-a review on recent trends and emerging perspectives," *Journal of Polymers and the Environment,* vol. 19, pp. 637-676, 2011.
[60] S. Agarwal, "Biodegradable polymers: Present opportunities and challenges in providing a microplastic-free environment," *Macromolecular Chemistry and Physics,* vol. 221, no. 6, p. 2000017, 2020.
[61] C. J. Bettinger and J. T. Borenstein, "Biomaterials-based microfluidics for engineered tissue constructs," *Soft Matter,* vol. 6, no. 20, pp. 4999-5015, 2010.
[62] G. Chen, T. Ushida, and T. Tateishi, "Hybrid biomaterials for tissue engineering: a preparative method for PLA or PLGA–collagen hybrid sponges," *Advanced Materials,* vol. 12, no. 6, pp. 455-457, 2000.
[63] H. K. Makadia and S. J. Siegel, "Poly lactic-co-glycolic acid (PLGA) as biodegradable controlled drug delivery carrier," *Polymers,* vol. 3, no. 3, pp. 1377-1397, 2011.
[64] M. Boaks *et al.*, "Biocompatible high-resolution 3D-printed microfluidic devices: integrated cell chemotaxis demonstration," *Micromachines,* vol. 14, no. 8, p. 1589, 2023.
[65] C. Warr *et al.*, "Biocompatible PEGDA resin for 3D printing," *ACS applied bio materials,* vol. 3, no. 4, pp. 2239-2244, 2020.
[66] M. Hakim Khalili *et al.*, "Mechanical behavior of 3D printed poly (ethylene glycol) diacrylate hydrogels in hydrated conditions investigated using atomic force microscopy," *ACS Applied Polymer Materials,* vol. 5, no. 4, pp. 3034-3042, 2023.
[67] S. N. Topkaya, "Gelatin methacrylate (GelMA) mediated electrochemical DNA biosensor for DNA hybridization," *Biosensors and Bioelectronics,* vol. 64, pp. 456-461, 2015.

[68] W. Eberhardt *et al.*, "Low cost fabrication technology for microfluidic devices based on micro injection moulding," *XP-002499487,* 2003.
[69] C. Dixon, J. Lamanna, and A. R. Wheeler, "Printed microfluidics," *Advanced Functional Materials,* vol. 27, no. 11, p. 1604824, 2017.
[70] P. Kim, K. W. Kwon, M. C. Park, S. H. Lee, S. M. Kim, and K. Y. Suh, "Soft lithography for microfluidics: a review," 2008.
[71] S. M. Scott and Z. Ali, "Fabrication methods for microfluidic devices: An overview," *Micromachines,* vol. 12, no. 3, p. 319, 2021.
[72] K. Karimi, A. Fardoost, N. Mhatre, J. Rajan, D. Boisvert, and M. Javanmard, "A Thorough Review of Emerging Technologies in Micro-and Nanochannel Fabrication: Limitations, Applications, and Comparison," *Micromachines,* vol. 15, no. 10, p. 1274, 2024.
[73] C. A. Baker, R. Bulloch, and M. G. Roper, "Comparison of separation performance of laser-ablated and wet-etched microfluidic devices," *Analytical and bioanalytical chemistry,* vol. 399, pp. 1473-1479, 2011.
[74] C. Iliescu, H. Taylor, M. Avram, J. Miao, and S. Franssila, "A practical guide for the fabrication of microfluidic devices using glass and silicon," *Biomicrofluidics,* vol. 6, no. 1, 2012.
[75] A. Waldbaur, H. Rapp, K. Länge, and B. E. Rapp, "Let there be chip—towards rapid prototyping of microfluidic devices: one-step manufacturing processes," *Analytical Methods,* vol. 3, no. 12, pp. 2681-2716, 2011.
[76] E. A. Waddell, "Laser ablation as a fabrication technique for microfluidic devices," *Microfluidic Techniques: Reviews and Protocols,* pp. 27-38, 2006.
[77] S. Shahriari, V. Patel, and P. R. Selvaganapathy, "Xurography as a tool for fabrication of microfluidic devices," *Journal of Micromechanics and Microengineering,* vol. 33, no. 8, p. 083002, 2023.
[78] S. Kojić *et al.*, "Optimization of hybrid microfluidic chip fabrication methods for biomedical application," *Microfluidics and Nanofluidics,* vol. 24, no. 9, p. 66, 2020.
[79] G. S. Fiorini and D. T. Chiu, "Disposable microfluidic devices: fabrication, function, and application," *BioTechniques,* vol. 38, no. 3, pp. 429-446, 2005.
[80] U. M. Attia, S. Marson, and J. R. Alcock, "Micro-injection moulding of polymer microfluidic devices," *Microfluidics and nanofluidics,* vol. 7, pp. 1-28, 2009.
[81] D. J. Guckenberger, T. E. De Groot, A. M. Wan, D. J. Beebe, and E. W. Young, "Micromilling: a method for ultra-rapid prototyping of plastic microfluidic devices," *Lab on a Chip,* vol. 15, no. 11, pp. 2364-2378, 2015.
[82] V. Faustino, S. O. Catarino, R. Lima, and G. Minas, "Biomedical microfluidic devices by using low-cost fabrication techniques: A review," *Journal of biomechanics,* vol. 49, no. 11, pp. 2280-2292, 2016.
[83] O. Skurtys and J. Aguilera, "Applications of microfluidic devices in food engineering," *Food Biophysics,* vol. 3, pp. 1-15, 2008.
[84] A. K. Au, W. Lee, and A. Folch, "Mail-order microfluidics: evaluation of stereolithography for the production of microfluidic devices," *Lab on a Chip,* vol. 14, no. 7, pp. 1294-1301, 2014.
[85] Y. Xia and G. M. Whitesides, "Soft lithography," *Angewandte Chemie International Edition,* vol. 37, no. 5, pp. 550-575, 1998.
[86] D. B. Wolfe, D. Qin, and G. M. Whitesides, "Rapid prototyping of microstructures by soft lithography for biotechnology," *Microengineering in Biotechnology,* pp. 81-107, 2009.

[87] W. Su, B. S. Cook, Y. Fang, and M. M. Tentzeris, "Fully inkjet-printed microfluidics: a solution to low-cost rapid three-dimensional microfluidics fabrication with numerous electrical and sensing applications," *Sci Rep,* vol. 6, no. 1, p. 35111, 2016.
[88] Y. Zhang, "Three-dimensional-printing for microfluidics or the other way around?," *IJB,* vol. 5, no. 2, 2019, doi: 10.18063/ijb.v5i2.192.
[89] G. Gonzalez, I. Roppolo, C. F. Pirri, and A. Chiappone, "Current and emerging trends in polymeric 3D printed microfluidic devices," *Additive Manufacturing,* vol. 55, p. 102867, 2022.
[90] R. Su, F. Wang, and M. C. McAlpine, "3D printed microfluidics: advances in strategies, integration, and applications," *Lab on a Chip,* vol. 23, no. 5, pp. 1279-1299, 2023.
[91] F. Li, N. P. Macdonald, R. M. Guijt, and M. C. Breadmore, "Increasing the functionalities of 3D printed microchemical devices by single material, multimaterial, and print-pause-print 3D printing," *Lab on a Chip,* vol. 19, no. 1, pp. 35-49, 2019.
[92] A. Tony *et al.*, "The additive manufacturing approach to polydimethylsiloxane (PDMS) microfluidic devices: review and future directions," *Polymers,* vol. 15, no. 8, p. 1926, 2023.
[93] V. Mehta and S. N. Rath, "3D printed microfluidic devices: a review focused on four fundamental manufacturing approaches and implications on the field of healthcare," *Bio-Design and Manufacturing,* vol. 4, no. 2, pp. 311-343, 2021.
[94] C. Chen, B. T. Mehl, A. S. Munshi, A. D. Townsend, D. M. Spence, and R. S. Martin, "3D-printed microfluidic devices: fabrication, advantages and limitations—a mini review," *Analytical Methods,* vol. 8, no. 31, pp. 6005-6012, 2016.
[95] J. Nam and M. Kim, "Advances in materials and technologies for digital light processing 3D printing," *Nano Convergence,* vol. 11, no. 1, p. 45, 2024.
[96] S. Swetha, T. J. Sahiti, G. S. Priya, K. Harshitha, and A. Anil, "Review on digital light processing (DLP) and effect of printing parameters on quality of print," *Interactions,* vol. 245, no. 1, p. 178, 2024.
[97] X. Wang *et al.*, "Advances in precision microfabrication through digital light processing: system development, material and applications," *Virtual and Physical Prototyping,* vol. 18, no. 1, p. e2248101, 2023.
[98] Z. Zhao, X. Tian, and X. Song, "Engineering materials with light: recent progress in digital light processing based 3D printing," *Journal of Materials Chemistry C,* vol. 8, no. 40, pp. 13896-13917, 2020.
[99] H. Li *et al.*, "Digital light processing (DLP)-based (bio) printing strategies for tissue modeling and regeneration," *Aggregate,* vol. 4, no. 2, p. e270, 2023.
[100] J. Zhang, Q. Hu, S. Wang, J. Tao, and M. Gou, "Digital light processing based three-dimensional printing for medical applications," *International journal of bioprinting,* vol. 6, no. 1, p. 242, 2019.
[101] M. Bifano, "Digital light processing: A review on the printing resolution and the materials options," *Appl Comput Eng,* vol. 1, pp. 17-25, 2022.
[102] N. Bhattacharjee, A. Urrios, S. Kang, and A. Folch, "The upcoming 3D-printing revolution in microfluidics," *Lab on a Chip,* vol. 16, no. 10, pp. 1720-1742, 2016.
[103] R. Amin *et al.*, "3D-printed microfluidic devices," *Biofabrication,* vol. 8, no. 2, p. 022001, 2016.

[104] S. Grebenyuk *et al.*, "Large-scale perfused tissues via synthetic 3D soft microfluidics," *Nature Communications,* vol. 14, no. 1, p. 193, 2023.
[105] J. Knoška *et al.*, "Ultracompact 3D microfluidics for time-resolved structural biology," *Nature communications,* vol. 11, no. 1, p. 657, 2020.
[106] H. J. McLennan *et al.*, "Nano-liter perfusion microfluidic device made entirely by two-photon polymerization for dynamic cell culture with easy cell recovery," *Sci Rep,* vol. 13, no. 1, p. 562, 2023.
[107] Y. Zhang *et al.*, "Real-time in-situ electrochemical monitoring of Pseudomonas aeruginosa biofilms grown on air–liquid interface and its antibiotic susceptibility using a novel dual-chamber microfluidic device," *Biotechnology and Bioengineering,* vol. 120, no. 3, pp. 702-714, 2023.
[108] A. M. Nightingale *et al.*, "Monitoring biomolecule concentrations in tissue using a wearable droplet microfluidic-based sensor," *Nature communications,* vol. 10, no. 1, p. 2741, 2019.
[109] C. Ye *et al.*, "A wearable aptamer nanobiosensor for non-invasive female hormone monitoring," *Nature nanotechnology,* vol. 19, no. 3, pp. 330-337, 2024.
[110] H. Li, A. Raza, S. Yuan, F. AlMarzooqi, N. X. Fang, and T. Zhang, "Biomimetic on-chip filtration enabled by direct micro-3D printing on membrane," *Sci Rep,* vol. 12, no. 1, p. 8178, 2022.
[111] B. Dai *et al.*, "Biomimetic apposition compound eye fabricated using microfluidic-assisted 3D printing," *Nature communications,* vol. 12, no. 1, p. 6458, 2021.
[112] M. Islam, R. Natu, and R. Martinez-Duarte, "A study on the limits and advantages of using a desktop cutter plotter to fabricate microfluidic networks," *Microfluidics and nanofluidics,* vol. 19, pp. 973-985, 2015.
[113] G. I. Salentijn, P. E. Oomen, M. Grajewski, and E. Verpoorte, "Fused deposition modeling 3D printing for (bio) analytical device fabrication: procedures, materials, and applications," *Analytical chemistry,* vol. 89, no. 13, pp. 7053-7061, 2017.
[114] W. H. Goh and M. Hashimoto, "Fabrication of 3D microfluidic channels and in-channel features using 3D printed, water-soluble sacrificial mold," *Macromolecular materials and engineering,* vol. 303, no. 3, p. 1700484, 2018.
[115] V. Saggiomo and A. H. Velders, "Simple 3D printed scaffold-removal method for the fabrication of intricate microfluidic devices," *Advanced science,* vol. 2, no. 9, p. 1500125, 2015.
[116] S. Regmi, C. Poudel, R. Adhikari, and K. Q. Luo, "Applications of microfluidics and organ-on-a-chip in cancer research," *Biosensors,* vol. 12, no. 7, p. 459, 2022.
[117] M. Sekhwama, K. Mpofu, S. Sivarasu, and P. Mthunzi-Kufa, "Applications of microfluidics in biosensing," *Discover Applied Sciences,* vol. 6, no. 6, p. 303, 2024.
[118] X. Wang *et al.*, "Microfluidics-based strategies for molecular diagnostics of infectious diseases," *Military Medical Research,* vol. 9, no. 1, p. 11, 2022.
[119] P. Lakhera, V. Chaudhary, B. Bhardwaj, P. Kumar, and S. Kumar, "Development and recent advancement in microfluidics for point of care biosensor applications: A review," *Biosensors and Bioelectronics: X,* vol. 11, p. 100218, 2022.
[120] J. B. Angell, S. C. Terry, and P. W. Barth, "Silicon micromechanical devices," *Scientific American,* vol. 248, no. 4, pp. 44-55, 1983.
[121] G. Casquillas and H. Timothée, "Introduction to lab on a chip 2015: review, history and future," ed, 2015.

[122] C. Zhang, J. Xu, W. Ma, and W. Zheng, "PCR microfluidic devices for DNA amplification," *Biotechnology advances,* vol. 24, no. 3, pp. 243-284, 2006.
[123] B. Karger, Y. Chu, and F. Foret, "Capillary electrophoresis of proteins and nucleic acids," *Annual review of biophysics and biomolecular structure,* vol. 24, pp. 579-610, 1995.
[124] X. Shao *et al.*, "Integrated proteome analysis device for fast single-cell protein profiling," *Analytical chemistry,* vol. 90, no. 23, pp. 14003-14010, 2018.
[125] H. Tavakoli *et al.*, "Recent advances in microfluidic platforms for single-cell analysis in cancer biology, diagnosis and therapy," *TrAC Trends in Analytical Chemistry,* vol. 117, pp. 13-26, 2019.
[126] N. Shembekar, H. Hu, D. Eustace, and C. A. Merten, "Single-cell droplet microfluidic screening for antibodies specifically binding to target cells," *Cell reports,* vol. 22, no. 8, pp. 2206-2215, 2018.
[127] R. Sanka, J. Lippai, D. Samarasekera, S. Nemsick, and D. Densmore, "3d μ f-interactive design environment for continuous flow microfluidic devices," *Sci Rep,* vol. 9, no. 1, p. 9166, 2019.
[128] J. H. Sung, "Pharmacokinetic-based multi-organ chip for recapitulating organ interactions," in *Methods in Cell Biology*, vol. 146: Elsevier, 2018, pp. 183-197.
[129] S. N. Bhatia and D. E. Ingber, "Microfluidic organs-on-chips," *Nature biotechnology,* vol. 32, no. 8, pp. 760-772, 2014.
[130] K. M. Bircsak *et al.*, "A 3D microfluidic liver model for high throughput compound toxicity screening in the OrganoPlate®," *Toxicology,* vol. 450, p. 152667, 2021.
[131] D. Huh *et al.*, "A human disease model of drug toxicity–induced pulmonary edema in a lung-on-a-chip microdevice," *Science translational medicine,* vol. 4, no. 159, pp. 159ra147-159ra147, 2012.
[132] N. Gupta, J. Liu, B. Patel, D. Solomon, B. Vaidya, and V. Gupta, "Microfluidics-based 3D cell culture models: utility in novel drug discovery and delivery research. Bioeng Transl Med 1 (1): 63–81," ed, 2016.
[133] C. Beaurivage *et al.*, "Development of a gut-on-a-chip model for high throughput disease modeling and drug discovery," *International journal of molecular sciences,* vol. 20, no. 22, p. 5661, 2019.
[134] I. Pediaditakis *et al.*, "A microengineered Brain-Chip to model neuroinflammation in humans," *Iscience,* vol. 25, no. 8, 2022.
[135] D. Cruz-Moreira *et al.*, "Assessing the influence of perfusion on cardiac microtissue maturation: A heart-on-chip platform embedding peristaltic pump capabilities," *Biotechnology and Bioengineering,* vol. 118, no. 8, pp. 3128-3137, 2021.
[136] M. Radisic, "From engineered tissues and microfludics to human eyes-on-a-chip," vol. 36, ed: Mary Ann Liebert, Inc., publishers 140 Huguenot Street, 3rd Floor New …, 2020, pp. 4-6.
[137] A. Grosberg, A. P. Nesmith, J. A. Goss, M. D. Brigham, M. L. McCain, and K. K. Parker, "Muscle on a chip: in vitro contractility assays for smooth and striated muscle," *Journal of pharmacological and toxicological methods,* vol. 65, no. 3, pp. 126-135, 2012.
[138] V. V. Thacker, N. Dhar, K. Sharma, R. Barrile, K. Karalis, and J. D. McKinney, "A lung-on-chip model of early Mycobacterium tuberculosis infection reveals an essential role for alveolar epithelial cells in controlling bacterial growth," *Elife,* vol. 9, p. e59961, 2020.

[139] P.-Y. Chen, M.-J. Hsieh, Y.-H. Liao, Y.-C. Lin, and Y.-T. Hou, "Liver-on-a-chip platform to study anticancer effect of statin and its metabolites," *Biochemical Engineering Journal,* vol. 165, p. 107831, 2021.
[140] E. C. Okpara, T. O. Ajiboye, D. C. Onwudiwe, and O. B. Wojuola, "Optical and electrochemical techniques for point-of-care water quality monitoring: a review," *Results in Chemistry,* vol. 5, p. 100710, 2023.
[141] P. Panda and S. Chakroborty, "Optical sensor technology and its application in detecting environmental effluents: a review," *International journal of environmental analytical chemistry,* vol. 104, no. 16, pp. 4057-4072, 2024.
[142] B. Jin *et al.*, "Upconversion fluorescence-based paper disc for multiplex point-of-care testing in water quality monitoring," *Analytica chimica acta,* vol. 1192, p. 339388, 2022.
[143] X. Chen *et al.*, "In situ and self-adaptive BOD bioreaction sensing system based on environmentally domesticated microbial populations," *Talanta,* vol. 261, p. 124671, 2023.
[144] D. Fahimi, O. Mahdavipour, J. Sabino, R. M. White, and I. Paprotny, "Vertically-stacked MEMS PM2. 5 sensor for wearable applications," *Sensors and Actuators A: Physical,* vol. 299, p. 111569, 2019.
[145] H. Sun, Y. Jia, H. Dong, L. Fan, and J. Zheng, "Multiplex quantification of metals in airborne particulate matter via smartphone and paper-based microfluidics," *Analytica Chimica Acta,* vol. 1044, pp. 110-118, 2018.
[146] M. Ueland *et al.*, "Capillary-driven microfluidic paper-based analytical devices for lab on a chip screening of explosive residues in soil," *Journal of Chromatography A,* vol. 1436, pp. 28-33, 2016.
[147] G. Luka *et al.*, "Microfluidics integrated biosensors: A leading technology towards lab-on-a-chip and sensing applications," *Sensors,* vol. 15, no. 12, pp. 30011-30031, 2015.
[148] V. Naresh and N. Lee, "A review on biosensors and recent development of nanostructured materials-enabled biosensors," *Sensors,* vol. 21, no. 4, p. 1109, 2021.
[149] P. Mehrotra, "Biosensors and their applications–A review," *Journal of oral biology and craniofacial research,* vol. 6, no. 2, pp. 153-159, 2016.
[150] S. Vigneshvar, C. Sudhakumari, B. Senthilkumaran, and H. Prakash, "Recent advances in biosensor technology for potential applications–an overview," *Frontiers in bioengineering and biotechnology,* vol. 4, p. 11, 2016.
[151] M. B. Kulkarni, N. H. Ayachit, and T. M. Aminabhavi, "Biosensors and microfluidic biosensors: from fabrication to application," *Biosensors,* vol. 12, no. 7, p. 543, 2022.
[152] K. E. Bates and H. Lu, "Optics-integrated microfluidic platforms for biomolecular analyses," *Biophysical journal,* vol. 110, no. 8, pp. 1684-1697, 2016.
[153] M. K. Alam *et al.*, "Recent advances in microfluidic technology for manipulation and analysis of biological cells (2007–2017)," *Analytica chimica acta,* vol. 1044, pp. 29-65, 2018.
[154] T. Q. Hung, W. H. Chin, Y. Sun, A. Wolff, and D. D. Bang, "A novel lab-on-chip platform with integrated solid phase PCR and Supercritical Angle Fluorescence (SAF) microlens array for highly sensitive and multiplexed pathogen detection," *Biosensors and Bioelectronics,* vol. 90, pp. 217-223, 2017.
[155] S. Ciampi, J. B. Harper, and J. J. Gooding, "Wet chemical routes to the assembly of organic monolayers on silicon surfaces via the formation of Si-

C bonds: Surface preparation, passivation and functionalization," *Chemical Society Reviews,* vol. 39, no. 6, pp. 2158-2183, 2010.
[156] J. Wang, Y. Ren, and B. Zhang, *Application of microfluidics in biosensors*. IntechOpen, 2020.
[157] H. Huang and D. Densmore, "Integration of microfluidics into the synthetic biology design flow," *Lab on a Chip,* vol. 14, no. 18, pp. 3459-3474, 2014.
[158] A. Bange, H. B. Halsall, and W. R. Heineman, "Microfluidic immunosensor systems," *Biosensors and Bioelectronics,* vol. 20, no. 12, pp. 2488-2503, 2005.
[159] H. Becker and C. Gärtner, "Polymer microfabrication methods for microfluidic analytical applications," *ELECTROPHORESIS: An International Journal,* vol. 21, no. 1, pp. 12-26, 2000.
[160] G. M. Whitesides, "The origins and the future of microfluidics," *Nature,* vol. 442, no. 7101, pp. 368-373, 2006/07/01 2006, doi: 10.1038/nature05058.
[161] S. K. Sia and L. J. Kricka, "Microfluidics and point-of-care testing," *Lab on a Chip,* vol. 8, no. 12, pp. 1982-1983, 2008.
[162] C. D. Chin, V. Linder, and S. K. Sia, "Commercialization of microfluidic point-of-care diagnostic devices," *Lab on a Chip,* vol. 12, no. 12, pp. 2118-2134, 2012.
[163] P. Ranjan, M. A. Sadique, A. Parihar, C. Dhand, A. Mishra, and R. Khan, "Commercialization of microfluidic point-of-care diagnostic devices," in *Advanced Microfluidics Based Point-of-Care Diagnostics*: CRC Press, 2022, pp. 383-398.
[164] P. Yager *et al.*, "Microfluidic diagnostic technologies for global public health," *Nature,* vol. 442, no. 7101, pp. 412-418, 2006.
[165] W. Gao *et al.*, "Fully integrated wearable sensor arrays for multiplexed in situ perspiration analysis," *Nature,* vol. 529, no. 7587, pp. 509-514, 2016.
[166] A. W. Martinez, S. T. Phillips, G. M. Whitesides, and E. Carrilho, "Diagnostics for the developing world: microfluidic paper-based analytical devices," ed: ACS Publications, 2010.
[167] X. Jin, C. Liu, T. Xu, L. Su, and X. Zhang, "Artificial intelligence biosensors: Challenges and prospects," *Biosensors and Bioelectronics,* vol. 165, p. 112412, 2020.
[168] I. Lee, D. Probst, D. Klonoff, and K. Sode, "Continuous glucose monitoring systems-Current status and future perspectives of the flagship technologies in biosensor research," *Biosensors and Bioelectronics,* vol. 181, p. 113054, 2021.
[169] C. Carrell *et al.*, "Beyond the lateral flow assay: A review of paper-based microfluidics," *Microelectronic Engineering,* vol. 206, pp. 45-54, 2019.
[170] H.-F. Tsai, S. Podder, and P.-Y. Chen, "Microsystem advances through integration with artificial intelligence," *Micromachines,* vol. 14, no. 4, p. 826, 2023.
[171] W. R. de Araujo, H. Lukas, M. D. Torres, W. Gao, and C. de la Fuente-Nunez, "Low-cost biosensor technologies for rapid detection of COVID-19 and future pandemics," *ACS nano,* vol. 18, no. 3, pp. 1757-1777, 2024.
[172] H. M. Fahmy *et al.*, "Recent progress in graphene-and related carbon-nanomaterial-based electrochemical biosensors for early disease detection," *ACS Biomaterials Science & Engineering,* vol. 8, no. 3, pp. 964-1000, 2022.
[173] N. O. Gomes, E. Carrilho, S. A. S. Machado, and L. F. Sgobbi, "Bacterial cellulose-based electrochemical sensing platform: A smart material for miniaturized biosensors," *Electrochimica Acta,* vol. 349, p. 136341, 2020.

[174] J. M. Mohan, K. Amreen, M. B. Kulkarni, A. Javed, S. K. Dubey, and S. Goel, "Optimized ink jetted paper device for electroanalytical detection of picric acid," *Colloids and Surfaces B: Biointerfaces,* vol. 208, p. 112056, 2021.
[175] R. Park, S. Jeon, J. Jeong, S.-Y. Park, D.-W. Han, and S. W. Hong, "Recent advances of point-of-care devices integrated with molecularly imprinted polymers-based biosensors: from biomolecule sensing design to intraoral fluid testing," *Biosensors,* vol. 12, no. 3, p. 136, 2022.
[176] Z. Asmare and M. Erkihun, "Recent application of dna microarray techniques to diagnose infectious disease," *Pathology and Laboratory Medicine International,* pp. 77-82, 2023.
[177] J. Yuan, X. Zhao, X. Wang, and Z. Gu, "Image decoding of photonic crystal beads array in the microfluidic chip for multiplex assays," *Sci Rep,* vol. 4, no. 1, p. 6755, 2014.
[178] L. Wang and P. C. Li, "Microfluidic DNA microarray analysis: A review," *Analytica chimica acta,* vol. 687, no. 1, pp. 12-27, 2011.
[179] P. Pattanayak *et al.*, "Microfluidic chips: recent advances, critical strategies in design, applications and future perspectives," *Microfluidics and nanofluidics,* vol. 25, pp. 1-28, 2021.
[180] E. C. Welch, J. M. Powell, T. B. Clevinger, A. E. Fairman, and A. Shukla, "Advances in biosensors and diagnostic technologies using nanostructures and nanomaterials," *Advanced Functional Materials,* vol. 31, no. 44, p. 2104126, 2021.
[181] J. Noor, A. Chaudhry, and S. Batool, "Microfluidic technology, artificial intelligence, and biosensors as advanced technologies in cancer screening: a review article," *Cureus,* vol. 15, no. 5, 2023.
[182] G. Lin, D. Makarov, and O. G. Schmidt, "Magnetic sensing platform technologies for biomedical applications," *Lab on a Chip,* vol. 17, no. 11, pp. 1884-1912, 2017.
[183] V. Nabaei, R. Chandrawati, and H. Heidari, "Magnetic biosensors: Modelling and simulation," *Biosensors and Bioelectronics,* vol. 103, pp. 69-86, 2018.
[184] R. Khan, A. Mohammad, and A. M. Asiri, *Advanced biosensors for health care applications*. Elsevier, 2019.
[185] G. Hernandez-Vargas, J. E. Sosa-Hernández, S. Saldarriaga-Hernandez, A. M. Villalba-Rodríguez, R. Parra-Saldivar, and H. M. Iqbal, "Electrochemical biosensors: A solution to pollution detection with reference to environmental contaminants," *Biosensors,* vol. 8, no. 2, p. 29, 2018.
[186] A. Hatamie, X. He, X.-W. Zhang, P. E. Oomen, and A. G. Ewing, "Advances in nano/microscale electrochemical sensors and biosensors for analysis of single vesicles, a key nanoscale organelle in cellular communication," *Biosensors and Bioelectronics,* vol. 220, p. 114899, 2023.
[187] I. Hernández-Neuta *et al.*, "Microfluidic magnetic fluidized bed for DNA analysis in continuous flow mode," *Biosensors and Bioelectronics,* vol. 102, pp. 531-539, 2018.
[188] J. Yu, H. Wu, L. He, L. Tan, Z. Jia, and N. Gan, "The universal dual-mode aptasensor for simultaneous determination of different bacteria based on naked eyes and microfluidic-chip together with magnetic DNA encoded probes," *Talanta,* vol. 225, p. 122062, 2021.
[189] A. Doostmohammadi, K. Youssef, S. Akhtarian, G. Kraft, and P. Rezai, "Fluorescent bacteria detection in water using cell imprinted polymer (CIP) coated microparticles in a magnetophoretic microfluidic device," *Talanta,* vol. 268, p. 125290, 2024.

[190] G. Barber and A. Arrott, "History and magnetics of compass adjusting," *IEEE Transactions on magnetics,* vol. 24, no. 6, pp. 2883-2885, 1988.
[191] H. Bray, *You are here: From the compass to GPS, the history and future of how we find ourselves*. Basic Books, 2014.
[192] J. Lenz and S. Edelstein, "Magnetic sensors and their applications," *IEEE Sensors journal,* vol. 6, no. 3, pp. 631-649, 2006.
[193] H. Weinstock, "SQUID sensors: fundamentals, fabrication and applications," 2012.
[194] Y. Développement, "Magnetic Sensor Market and Technologies Report from Yole Développement. 2017," ed.
[195] G. Kokkinis, S. Cardoso, F. Keplinger, and I. Giouroudi, "Microfluidic platform with integrated GMR sensors for quantification of cancer cells," *Sensors and Actuators B: Chemical,* vol. 241, pp. 438-445, 2017.
[196] M. Julliere, "Tunneling between ferromagnetic films," *Physics letters A,* vol. 54, no. 3, pp. 225-226, 1975.
[197] N. A. Wibowo, C. Kurniawan, D. K. Kusumahastuti, A. Setiawan, and E. Suharyadi, "Potential of tunneling magnetoresistance coupled to iron oxide nanoparticles as a novel transducer for biosensors-on-chip," *Journal of The Electrochemical Society,* vol. 171, no. 1, p. 017512, 2024.
[198] B. D. Fairbanks, M. P. Schwartz, C. N. Bowman, and K. S. Anseth, "Photoinitiated polymerization of PEG-diacrylate with lithium phenyl-2, 4, 6-trimethylbenzoylphosphinate: polymerization rate and cytocompatibility," *Biomaterials,* vol. 30, no. 35, pp. 6702-6707, 2009.
[199] T. Tamura and T. Suzuki, "Seamless fabrication technique for micro to millimeter structures by combining 3D printing and photolithography," *Japanese Journal of Applied Physics,* vol. 58, no. SD, p. SDDL10, 2019.
[200] N. Ghahremani Arekhloo *et al.*, "Motion artifact variability in biomagnetic wearable devices," *Frontiers in Medical Technology,* vol. 6, p. 1457535, 2024.
[201] S. Garcia-Rey, J. B. Nielsen, G. P. Nordin, A. T. Woolley, L. Basabe-Desmonts, and F. Benito-Lopez, "High-resolution 3D printing fabrication of a microfluidic platform for blood plasma separation," *Polymers,* vol. 14, no. 13, p. 2537, 2022.